Ecological Indicators 96 (2019) 174–191

Contents lists available at ScienceDirect

Ecological Indicators

journal homepage: www.elsevier.com/locate/ecolind

Detection of changes in shallow coral reefs status: Towards a spatial approach using hyperspectral and multispectral data

Touria Bajjouk[a,*], Pascal Mouquet[b], Michel Ropert[c], Jean-Pascal Quod[d], Ludovic Hoarau[c,e], Lionel Bigot[f], Nicolas Le Dantec[g,h], Christophe Delacourt[h], Jacques Populus[a]

[a] IFREMER Centre de Brest, DYNECO/LEBCO, BP 70, 29280 Plouzané, France
[b] Université de La Réunion/UMR ESPACE-DEV, Antenne SEAS-OI, 40 Avenue de Soweto, 97410 Saint-Pierre, La Réunion, France
[c] IFREMER, Délégation océan Indien, Rue Jean BERTHO, BP60, 97822 Le Port, La Réunion, France
[d] Pareto, 15 Impasse des Hyménées, 97438 Sainte Marie, La Réunion, France
[e] 3R: Rehabilitation of Réunion Island Reef, 97435 Saint-Paul, La Réunion, France
[f] UMR 9220 ENTROPIE, Université de La Réunion, IRD, CNRS, Laboratoire d'Excellence CORAIL, BP 7151, 97715 Saint Denis Cedex 9, La Réunion, France
[g] CEREMA—Centre d'Etudes et d'expertise sur les Risques, l'Environnement, la Mobilité et l'Aménagement, DTecEMF, 29280 Plouzané, France
[h] Laboratoire Géosciences Océan—UMR 6538, Université de Bretagne Occidentale, IUEM, Technopôle Brest-Iroise, Rue Dumont D'Urville, 29280 Plouzané, France

ARTICLE INFO

Keywords:
Change detection
Coral to Algae Index
Hyperspectral
Reef geomorphology
Remote sensing monitoring
Reunion Island

ABSTRACT

Coral reef degradation due to environmental change, including anthropogenic disturbances, is a major concern worldwide. Detecting and assessing both temporal and spatial changes in benthic cover is a crucial requirement to inform policy makers and guide conservation measures. Here, we introduce a spatial approach based on high resolution multispectral and hyperspectral image analysis, developed in order to detect and quantify changes in benthic cover in a highly heterogeneous shallow coral reef flat in Reunion Island in the South-West Indian Ocean. We propose a new index called HCAI (Hyperspectral Coral to Algae Index), defined as the ratio of living coral cover to the sum of living coral and algal covers. Benthic cover estimates were derived from airborne hyperspectral image processing using water column correction and unmixing models implemented with the four main coral reef benthic components: corals, algae, seagrass and sand. Ground truth and LIDAR data acquired simultaneously were used to validate processing accuracy. A significant positive correlation (adjusted $R^2 = 0.72$, p-value < 0.001) was obtained between coral cover recorded *in situ* and estimated from image analysis. Moreover, 13 habitat classes based on the four main benthic component covers were mapped at a scale of an entire reef. Diachronic analyses of hyperspectral images between 2009 and 2015 revealed an overall decrease of the HCAI index and a decrease in the area of all the dominant coral classes along the reef (-28.24% for the *coral* class for example), while the area of habitat classes dominated by algae strongly increased during the same period. Moreover, we detected and documented the spatial and temporal evolutions of coral geomorphological features composed with coral rubble deposits called *rubble tongues* (RTs) using different available sensors (i.e. hyperspectral, satellite, and orthophotography). Since 2003, four detected (RTs) have spread shoreward at a mean rate of 8.4 $m.y^{-1}$ including significant loss of reef structural complexity and heterogeneity, a spreading pattern which was confirmed by 2009 and 2015 hyperspectral data. Remote sensing and more specifically airborne hyperspectral approaches open new perspectives for coral reef monitoring, at high temporal and spatial resolutions.

1. Introduction

Coral reefs are one of the most complex, biodiverse, and productive ecosystems on the planet, playing a major social, economic and cultural role for millions of people (Spalding et al., 2017). These ecosystems also constitute a natural and physical barrier against storm-induced coastal hazards, in particular hurricanes, by significantly reducing wave energy (Ferrario et al., 2014; Guannel et al., 2016). However, coral reefs are also considered among the most vulnerable marine ecosystems (Bellwood et al., 2004; Halpern et al., 2007), facing increasing anthropogenic stressors and disturbances such as climate change, rising sea-surface temperatures, ocean acidification, soil erosion, pollution, and overfishing (Bozec and Mumby, 2014; Harborne et al., 2017). The global degradation of coral reefs has become a worldwide concern over

* Corresponding author.
E-mail address: touria.bajjouk@ifremer.fr (T. Bajjouk).

https://doi.org/10.1016/j.ecolind.2018.08.052
Received 24 January 2018; Received in revised form 26 June 2018; Accepted 24 August 2018
1470-160X/ © 2018 Elsevier Ltd. All rights reserved.

the two last decades (Hughes et al., 2017), emphasizing the urgent need for developing adequate tools to assess reef state and quality at large scales in order to propose adequate management strategies for mitigation of coral reef degradation and promoting resilience.

Management of coral reef seascapes requires an assessment of temporal variations driven by natural fluctuation, extreme disturbances such as cyclones and flood plumes (Perry et al., 2008) and by human activities. Monitoring programs can detect such change and help to understand the spatial and temporal dynamics of reef degradation and recovery, from global (Wilkinson, 2008) to local perspectives (Done et al., 2007). The most common methods used to detect temporal change in health status in the framework of reef monitoring programs are the Line or Point Intercept Transect (LIT and PIT) and Quadrats (Facon et al., 2016). Although these methods provide reliable results to quantify spatial and temporal benthic reef variations, change is often measured at small standardized scales and therefore reflects only a partial picture of the entire reef (Madin and Madin, 2015). Constrained by the accessibility of certain reef flat zones, these methods characterize a limited linear inner reef flat and therefore fail at taking into account important spatial heterogeneities of benthic communities distributed along an entire coral reef. In addition, they fail to detect geomorphological dimensions of the reef over decadal time scales. Given that coral reef organisms are affected by a wide range of processes that span scales from the cell up to thousands of kilometers (Allemand et al., 2011), proper assessment of the ecological state of the reef requires monitoring schemes that provide a comprehensive picture of coral reef structure and dynamics.

High resolution remote sensing is a suitable technique for evaluating the current trends of coral reef structure and its dynamics at larger spatial scales. Hedley et al. (2016) recently reviewed remote sensing techniques for monitoring and management of coral reefs and concluded that recent advances in sensors and processing have great potential to generate high resolution coral reef maps that incorporate various data sources in order to propose effective conservation management measures. The most common techniques applied to detect the nature and extent of land cover changes have used LANDSAT multispectral images (Andréfouët et al., 2001). However, the spatial resolution (i.e. tens of meters) of this sensor is not suitable for capturing the change in the dynamics of coral reef ecological status. Coral reef state requires monitoring at fine spatial scales in shallow waters, but currently, at this spatial resolution, most studies addressing detection of change are limited to geomorphological features. Recently, WorldView-3 satellite images were used to quantify live coral cover (LCC) using a band ratio-based index (Huang et al., 2018), however this index strongly depends on field surveyed LCCs. In addition to the spatial and spectral limitations of these two satellite sensors, Andréfouët (2012) draws attention to the issue of manual and therefore subjective boundary definitions along reef flat gradients. Furthermore, satellite-based methods often require substantial field surveys for characterization and validation of the detected benthic components (Hedley et al., 2016).

Field studies have demonstrated the ability of using narrow spectral bands to discriminate between *in situ* hyperspectral reflectance measurements of corals and algae (Hochberg and Atkinson, 2000; Karpouzli et al., 2004) and healthy corals (Holden and LeDrew, 1998). As an alternative to multispectral satellite images, hyperspectral imagery can be used to implement detection of change in coral reef status, with greater potential for discriminating benthic components. Airborne hyperspectral sensors provide sufficiently high spectral resolution to achieve good discrimination of the seabed types, and sub-meter spatial resolution to reveal distribution patterns at the fine scale of coral communities (Hochberg and Atkinson, 2000; Mishra et al., 2007). Andréfouët et al. (2004) used Compact Airborne Spectrographic Imager (CASI) data to demonstrate spectral differences between algae and corals. Joyce et al. (2013) recently tested a spectral index for mapping live coral cover using CASI-2 airborne hyperspectral imagery. Using hyperspectral images, Garcia et al. (2018) developed a lookup table (LUT) based approach to retrieve bottom depth and reflectance, with the latter used in benthic classification. They showed that the developed classification scheme enhances benthic classification and formulated the need of its application to other regions to evaluate its portability. All of these studies demonstrate an improvement in terms of discrimination of benthic components when employing airborne hyperspectral imaging to characterize coral reefs.

One of the acknowledged difficulties when using remote sensing applied to coral reef environments is spatial resolution (Garcia et al., 2018; Holden and LeDrew, 2001; Karpouzli et al., 2004). Small patches remain within a pixel size even with fine resolution (Kobryn et al., 2013), so the structural complexity of coral reefs leads to problems with mixed pixels as a result of high spatial heterogeneity. Addressing the issue of mixed pixels using would require classifying not only biologically uniform benthic components, but also pixels with a realistic mix of component types occurring in coral reefs (Petit et al., 2017). The accuracy of image geometric registration could also be a concern in the context of change detection based on remote sensing data (Garcia et al., 2014). Change detection algorithms may result in false estimates of change, especially in the areas of rapid spatial variation such as edges. Even if this issue can be accounted for by using spatial–contextual information contained in the neighborhood of each pixel (Coppin et al., 2004), it would be important to explore the possibility of developing change detection techniques that can bypass the registration process constraint and defect.

In Reunion Island (South-West Indian Ocean), coral reef monitoring programs are being carried out as part of the Global Coral Reef Monitoring Network (GCRMN) that started in 1998 (Chabanet et al., 2002), the Reef Check initiatives and the Water Framework Directive (WFD). Given the high heterogeneity of coral reef communities in shallow waters (Scopélitis et al., 2009), and their proximity to land, large scale surveys of the whole shoreward reef area would allow evaluation of impacts in areas that are difficult to access and that are likely most exposed to damage and human impacts. To our knowledge, only one study to date has attempted to detect coral reef community change on Reunion Island at Saint-Leu reef by integrating *in situ* and manual delineation of remote sensing data (Scopélitis et al., 2009). Even if this study provided an improved basis for judging the status of the coral communities, the coral cover, regarded as the most efficient indicator of coral reef health (Huang et al., 2018), could not be evaluated over time for the entire reef.

Using a spatial approach based on high resolution multispectral and hyperspectral image analysis, the present study aims to draw, for the first time, a baseline of current coral reef status in Saint-Gilles, a highly heterogeneous shallow reef flat in Reunion Island, that complements observations recorded with conventional *in situ* methods. The first objective was to develop an automatic image processing methodology which could be repeated over time to extract accurate spatial quantitative metrics on benthic coral reefs. Coral reef health status was evaluated through coral cover estimates and a new index called Hyperspectral Coral to Algae Index (HCAI), in addition to geomorphological features of the reef. A second objective was to illustrate, through a diachronic analysis between 2009 and 2015, the value of hyperspectral and multispectral imagery in quantifying spatial-temporal changes for metrics extracted using the developed method. Previously identified issues related to mixed pixels and limitations in geometric registration accuracy were taken into account by using respectively unmixing models and post-processing techniques. A benthic classification map was also generated for the Saint-Gilles reef flat which revealed consistency with the observed variations in habitat distribution. We demonstrate that such techniques open new opportunities for evaluating coral reef flat status at large spatial scales.

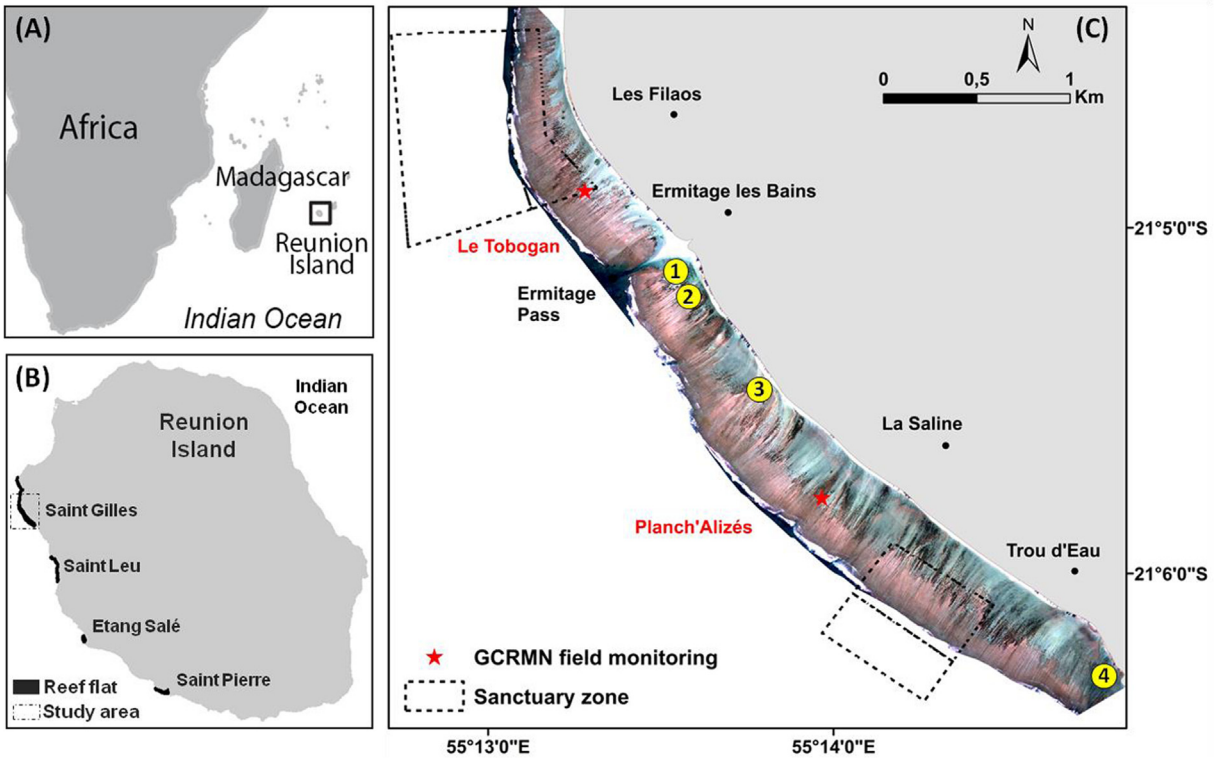

Fig. 1. Location of the Saint-Gilles reef unit studied site (C) in the Reunion Island fringing reef (B). True color image represents RGB hyperspectral image (C). Numbers indicate the location of the four investigated rubble tongues.

2. Materials and methods

2.1. Study site

Reunion Island is a volcanic island located at 55°29′E longitude and 21° 53′S latitude in the southwestern Indian Ocean. The island is under the influence of the Southern Equatorial Current which brings warm waters from the east, with annual sea surface temperatures varying between 21 °C and 27 °C. Current reef formations constitute a discontinuous belt with a total length of 25 km on the west leeside of the island (Fig. 1).

Saint Gilles study site (Fig. 1) is about 9 km long by 500 m wide reef flat located within the Reunion National Marine Reserve (RNMR). The Saint-Gilles reef is characterized by various types of coral reef habitats from near to offshore with successively a soft substrate back reef zone, a reef flat (or inner reef), a reef crest (wave breaking zone) and a reef slope (or outer reef) structured by many spurs and grooves. The fringing reef is characterized by very shallow depth and is partially exposed at low tide (0.90 m tidal amplitude). It is largely made up of massive and incrusting corals forms (*Porites* spp.) due to the high energy in this area. The inner reef flat hosts colonies of branching corals *Acropora muricata* and *Montipora* spp. *Millepora* spp. are found in the back reef area which can extend to the shoreline (Naim, 1993).

The Saint-Gilles reef unit can be split into three sub-units from north to south as described by Cordier (2007):

(1) A northern part featuring a narrow fringing reef (100 to 200 m wide) that widens southward as it approaches Ermitage Pass. This sub-unit is characterized by a low, almost non-existent back reef development.
(2) In the center, the Ermitage sub-unit is interrupted at its center by Ermitage Pass which is an extension of a gully. It is roughly 2 km long and up to 400 m wide.
(3) The last reef sub-unit is La Saline that extends to the south of "Trou d'Eau" where it is interrupted by basaltic rocks from the shore. Approximately 3.5 km long, with the same orientation as the Ermitage sub-unit, (trending northwest to southeast), and a maximum width of 600 m. This sub-unit has the most developed back reef of the Saint-Gilles reef, reaching up to 250 m wide.

2.2. Data acquisition

2.2.1. Airborne and satellite data

To characterize and quantify the changes in RI (Reunion Island) coral reef habitats and reef features, different types of imagery were used (Table 1).

Airborne hyperspectral data were acquired over the RI reef during two different projects:

(i) SPECTRHABENT-OI project in 2009 as part of the Litto3D program led by the French Hydrographic Survey (SHOM) and the National Institute of Geographic and Forest Information (IGN). Hyperspectral images were acquired using a Hyspex VNIR-1600 sensor that measures radiance between 406 nm and 994 nm with spectral and spatial resolutions of respectively 4 nm and 0.4 m. (ii) HYSCORES project in May 2015 using an AISA Eagle 1 k system. Hyperspectral images were acquired with spatial and spectral resolutions of resp. 0.4 m and 8 nm between 393 nm and 963 nm. Atmospheric correction was performed using measured spectral reflectance of different invariant ground targets acquired with an ASD hand-held spectroradiometer. The hyperspectral datasets were orthorectified with an RMS error of about 1 m.

To analyze the displacement of the rubble tongues (coral rubble shaped deposits on a coral reef platform) between 2003 and 2017, hyperspectral images were supplemented with high spatial resolution aerial photograph and satellite images from Pleiades (Appendix A, Table 1).

Lidar data were acquired over Reunion in June 2009 with a Hawkeye II instrument as part of the Litto3D framework. Lidar point

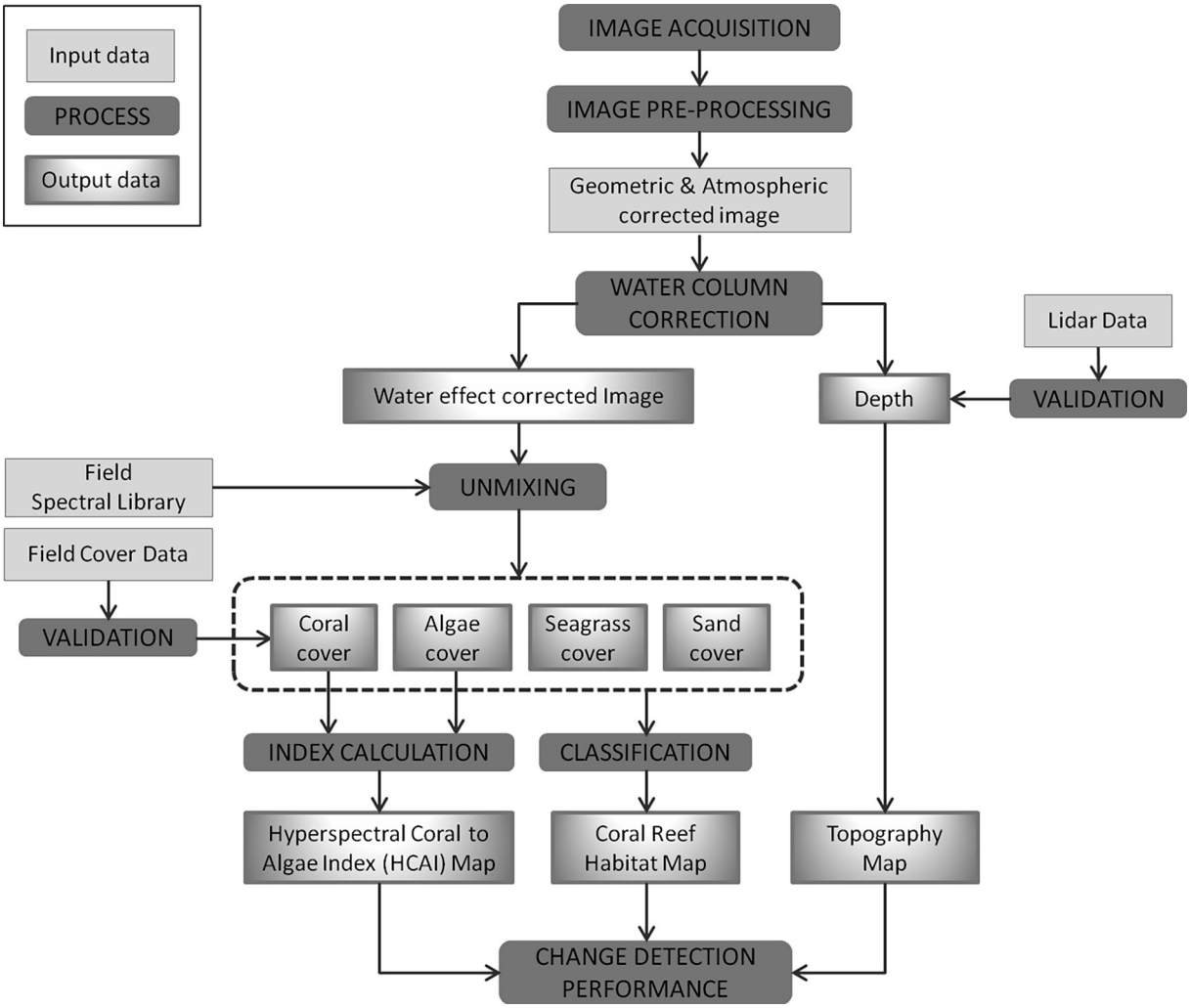

Fig. 2. Hyperspectral image processing workflow to perform coral reef change detection.

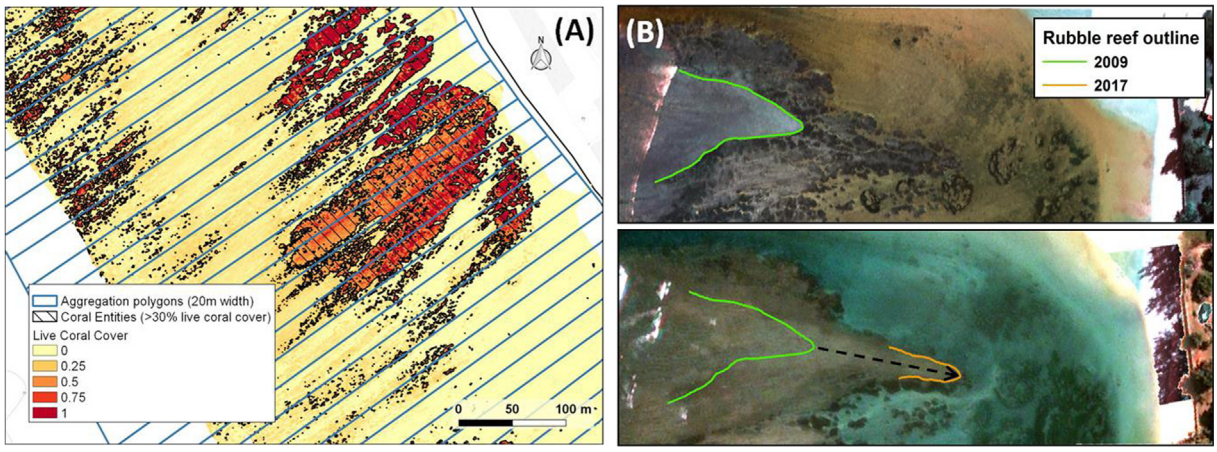

Fig. 3. Methodological approaches used to quantify coral reef changes, using coral entities (pixel to pixel approach) or 20 m width polygons (aggregation approach) to summarize the coral cover data (A). Position of the rubble tongue "RT1" in 2009 and 2017 (B). The black arrow shows the progress of the rubble limit between 2009 and 2017.

clouds provide depth maps with a vertical accuracy of 0.5 m.

2.2.2. Ground-truth data

Field surveys were performed in 2011 and 2015 across Saint-Gilles reef flats. A total of 37 control points were visited by scuba divers during the 2015 (hyperspectral) image acquisition. Each point was localized using GPS coordinates at the center of homogeneous areas of interest, five times larger than the geometric uncertainty of GPS measurements (3 m), therefore ensuring their representativeness and allowing positional error attenuation (Kobryn et al., 2013).

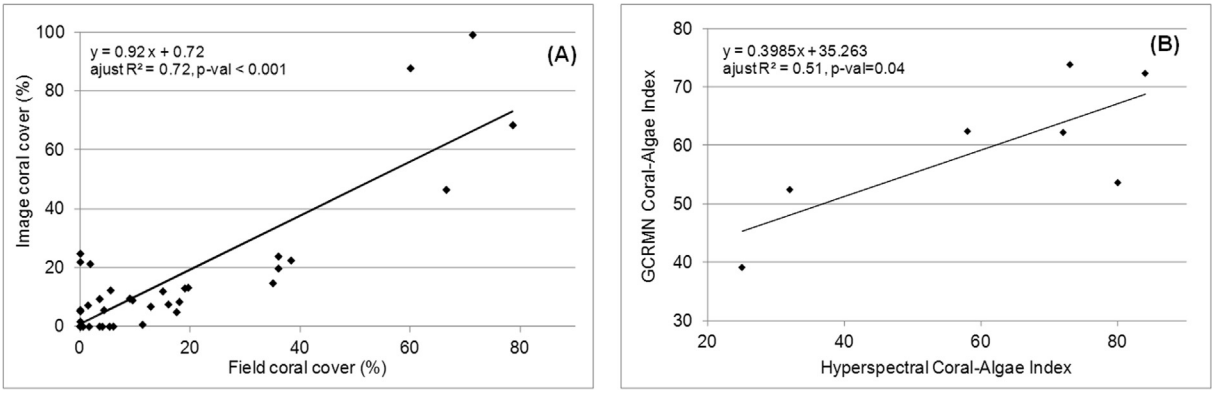

Fig. 4. Comparison between Saint-Gilles reef flat field coral cover and image estimated cover (A) and comparison of coral to algae index between GCRMN field monitoring and hyperspectral estimation (B).

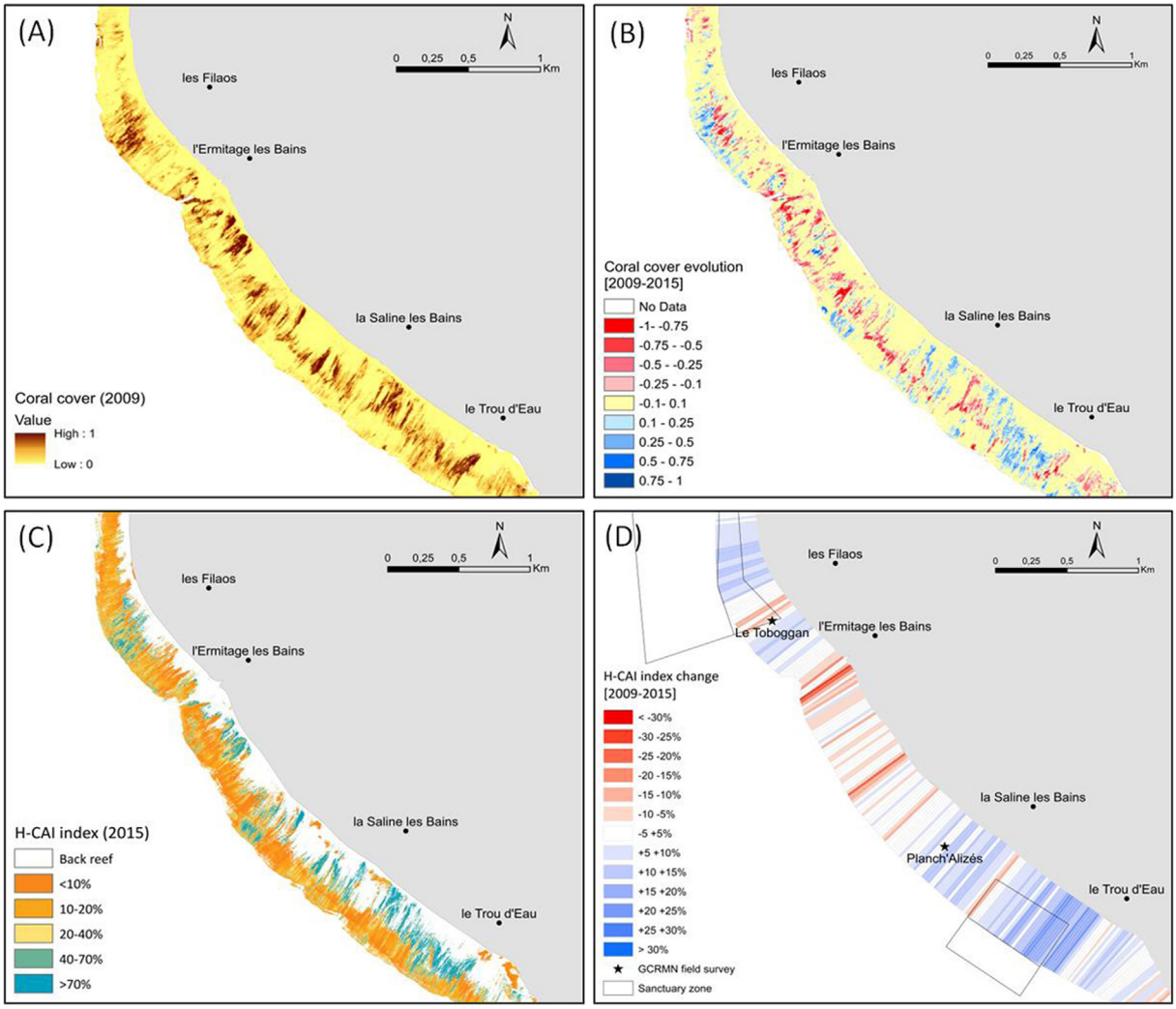

Fig. 5. Outputs obtained from hyperspectral imagery acquired on Saint-Gilles reef flat: Coral cover obtained for 2009 (A) and its change (B), Hyperspectral Coral to Algae Index HCAI (C) and its change between 2009 and 2015 aggregated into 20 m width polygons (D).

Parameters related to the benthic composition of the reef habitats and more specifically the benthic cover rates of the main biological components (algae, corals, seagrass) were visually estimated by 2 trained operators. Visual estimates of benthic covers provide a fast and reliable technique to estimate cover rates with the same level of accuracy as traditional survey methods like the LIT (Wilson et al., 2007). Efforts were made to cover a wide range of ecologically diverse areas of the reef taking into account access constraints.

2.2.3. Global Coral Reef Monitoring Network data

Since 1998, a standardized protocol from the GCRMN has been used for annual coral reef monitoring. This protocol aims to consolidate knowledge on coral reefs and their spatio-temporal trends in different areas around the world. It has been applied on 14 stations by the RNMR

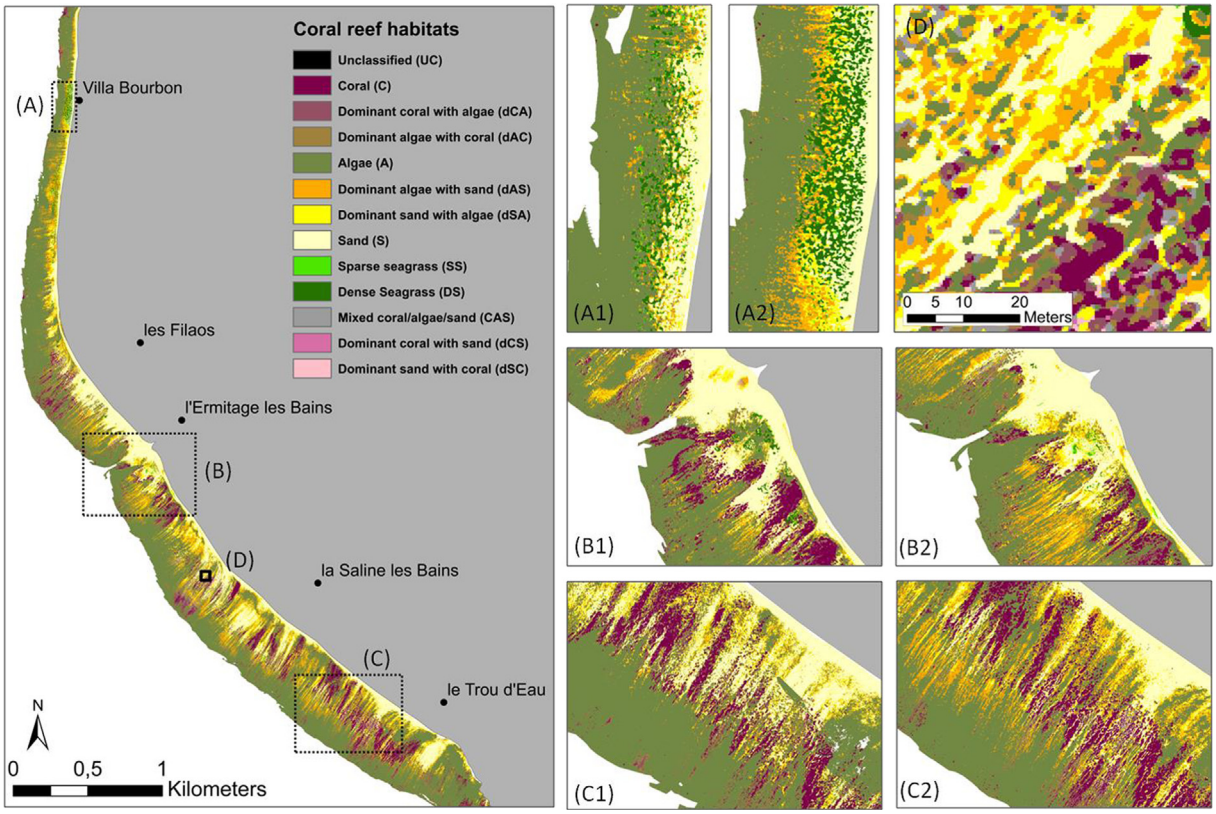

Fig. 6. Evolution of coral reef habitat classes between 2009 (1) and 2015 (2) for three zones (A, B, and C) of the Saint-Gilles coral reef unit. To the left, habitat map for the entire Saint-Gilles reef flat unit from 2015 image processing. (D) Picture represents a magnified full-resolution view of the map to illustrate the high level of heterogeneity in Saint-Gilles reef.

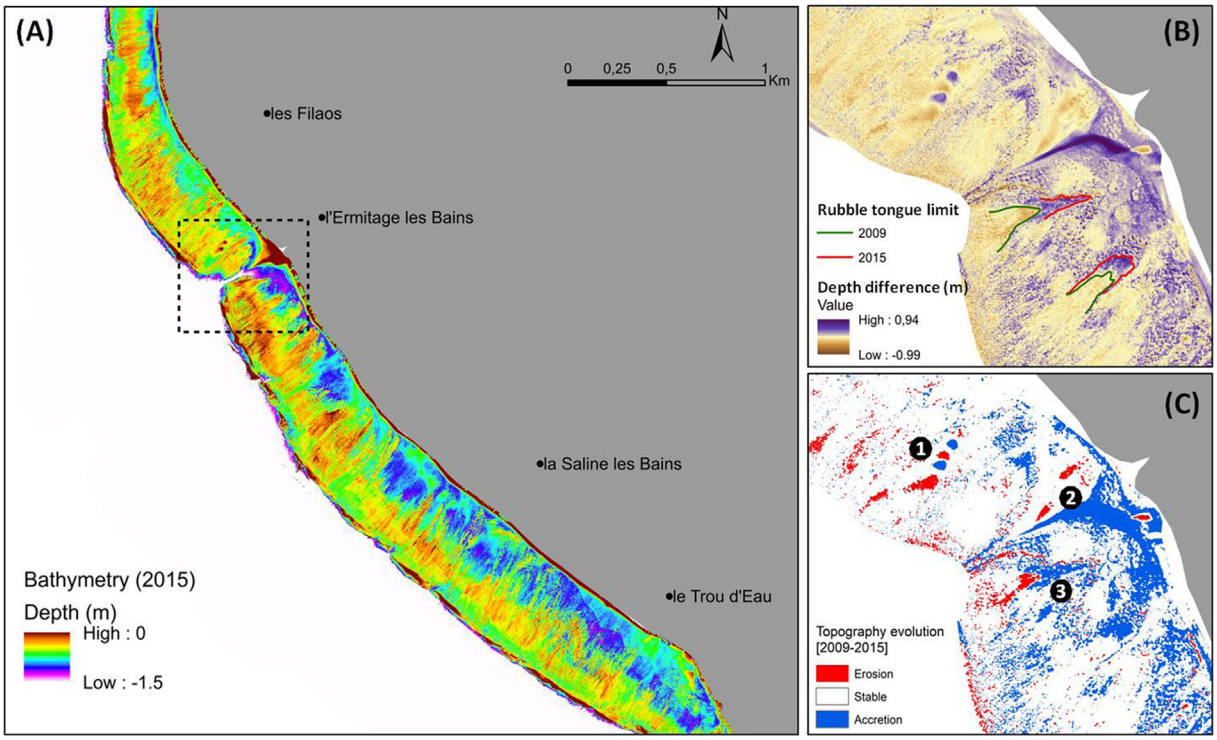

Fig. 7. Digital elevation model extracted from the 2015 hyperspectral image (A), differential bathymetry and the delineation of rubble tongues RT01 and RT02 (B) and topographic change estimated between 2009 and 2015 (C) in the Ermitage Pass area (dashed box). Numbers indicate the main identified geomorphologic features.

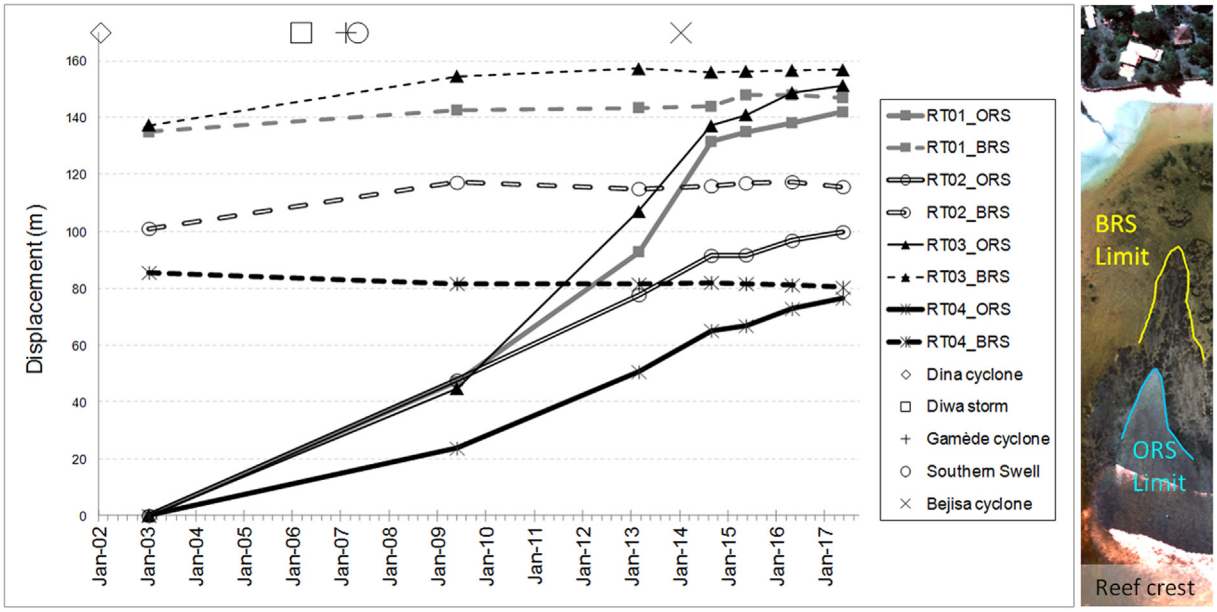

Fig. 8. The four studied rubble tongue (RT) displacements between 2003 and 2017 in the Saint-Gilles reef unit, with respect to live coral reef belt limits. Solid lines represent the outer reef side (ORS) limit. Dashed lines represent the back reef side (BRS) limit.

(Bigot et al., 2016). The two surveyed stations Toboggan and Planch'Alizés fall inside our study area.

2.3. Hyperspectral image data processing

The image processing procedure, as illustrated in the workflow diagram (Fig. 2) consists in 2 main steps. First, the hyperspectral images are inversed to retrieve depth and benthic substrate type using well-documented and tested methods. Then the validated benthic types are used to generate classification maps and compute indexes to perform change in different coral reef features. The implemented algorithms were based on the radiative transfer model inversion coupled with unmixing models commonly used in the past two decades for hyperspectral applications (Bioucas-Dias et al., 2012; Lee et al., 1998; Petit et al., 2017). Geometric and atmospheric corrections were performed prior to image processing. Since a visual examination of the atmospherically corrected images did not reveal any significant sun glint effect, no sun glint correction was applied to the images.

2.3.1. Water column correction

The water column correction applied for retrieving bottom reflectance data was based on the following simplified equation for signal attenuation derived from Lee's model (1998):

$$R_\lambda = R_{\infty,\lambda} + (R_{0,\lambda} - R_{\infty,\lambda}).\, e^{-2K_\lambda.H} \quad (1)$$

where

- o R_λ is the water surface reflectance at wavelength λ,
- o $R_{\infty,\lambda}$ is the reflectance of an infinite ocean depth at wavelength λ,
- o $R_{0,\lambda}$: is the seabed albedo at wavelength λ,
- o K_λ is the attenuation coefficient representing attenuation of the downwelling stream and the upwelling stream at wavelength λ, and
- o H is water depth (m).

For the attenuation coefficient (K_λ), considered to be constant spatially and over time, we used measured values from a radiometric survey conducted at the Hermitage Pass in 2015 using an irradiance sensor (Ramses TriOS), to process the 2009 and 2015 hyperspectral imagery. The reflectance at infinite depth ($R_{\infty,\lambda}$) was determined for each image by taking the measured reflectance values in a portion of image with sufficient water depth (H > 50 m), so that the seabed albedo contribution is zero.

2.3.2. Bathymetry retrieval

The estimation of water depth, last input needed to resolve Eq. (1), relies on its strong correlation with the reflectance values of the hyperspectral images in the near infrared, which has been observed for very shallow depths (between 0 and about 2 m). More specifically, in that depth range, reflectance in the 714–720 nm wavelength band depends mainly on the bathymetry, following an exponential relation (Eq. (2)), and less on the nature of the seabottom:

$$H_{hs} = \frac{1}{2K_{\lambda=714nm}} \ln\left(\frac{R_{0,\lambda=714nm}}{R_{\lambda=714nm}}\right) \quad (2)$$

where H_{hs} is the height of the water column for a given pixel.

The bathymetry is obtained as the difference between a reference water level, considered to be constant within each flight line, and the estimated water depth. The quality of the hyperspectral bathymetry estimation was validated by comparing the results obtained from processing the 2009 hyperspectral imagery with LIDAR data acquired simultaneously.

2.3.3. Benthic cover estimate

After seabed reflectance has been obtained, the cover rates of the main seabed components are determined by a spectral linear unmixing technique (Bioucas-Dias et al., 2012). The reflectance of a pixel is considered as the result of the weighted average of the reflectance values of the pure endmembers constituting the pixel, the weight of each endmember being proportional to their cover rate at that pixel. In Reunion Island reef areas, seabed type is composed of four ultra-dominant endmembers: sand, algae, coral, or seagrass. Spectral measurements were carried out *in situ* for these four endmembers in order to build the reference spectral library for the unmixing processing step. Spectral diversity was taken into account by selecting a relatively wide range of spectra for each endmember (Appendix B).

Spectral unmixing was performed using the IDL CONSTRAINED_MIN optimization algorithm (Windward Technologies, 1997). We chose the "Least Square" estimation as cost function, because it is the optimal unbiased estimator. Cover rate maps were thus obtained for

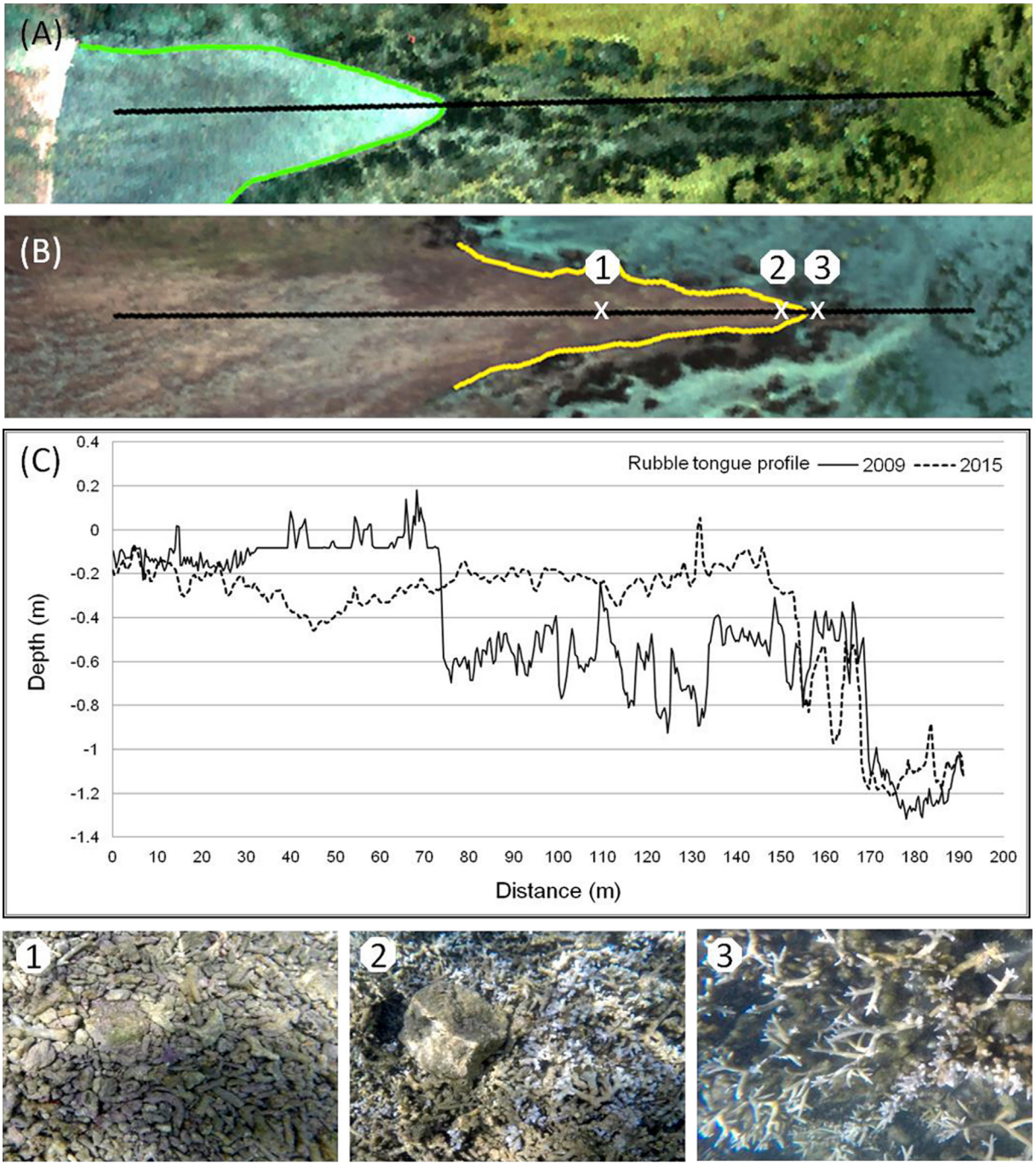

Fig. 9. 2009 (A) and 2015 (B) RVB images showing the rubble tongue RT01 overlain with a line representing its topographic profiles (C). Field pictures were acquired at the numbered positions indicated on (B) with respectively rubble (1), broken coral and rubbles (2), and live coral (3).

Table 1
Imagery data used for coral reef change detection assessment and mapping on Reunion Island.

Date	Sensor	Resolution (m)	*In situ* observations
23/01/2003	Aerial orthophotography IGN	0.10	
03/06/2009	Lidar sensor	1.00	
03/06/2009	Airborne hyperspectral imagery	0.40	x
05/03/2013	Satellite image (Pleiade)	0.50	
02/09/2014	Satellite image (Pleiade)	0.50	
22/05/2015	Airborne hyperspectral imagery	0.40	x
04/05/2016	Satellite image (Pléïades)	0.50	
22/05/2017	Satellite image (Pléïades)	0.50	

Table 2
Classes selected for coral reef habitat classification and their criteria (values are given in %).

ID	Coral reef habitat classes	Criteria (%)
SS	Sparse seagrass bed	33 < Seagrass < 66.7
DS	Dense seagrass bed	Seagrass > 66.7
C	Coral	Coral > 66.7
A	Algae	Algae > 66.7
S	Sand	Sand > 66.7
dCA	Dominant coral with algae	50 < Coral < 66.7 and Algae > Sand OR Coral < 50 and Algae < 50 and Sand < 16.7 and Coral > Algae
dCS	Dominant coral with sand	50 < Coral < 66.7 and Sand > Algae OR Coral < 50 and Sand < 50 and Algae < 16.7 and Coral > Sand
dAC	Dominant algae with coral	50 < Algae < 66.7 and Coral > Sand OR Algae < 50 and Coral < 50 and Sand < 16.7 and Algae > Coral
dAS	Dominant algae with sand	50 < Algae < 66.7 and Sand > Coral OR Algae < 50 and Sand < 50 and Coral < 16.7 and Algae > Sand
dSA	Dominant sand with algae	50 < Sand < 66.7 and Algae > Coral OR Algae < 50 and Sand < 50 and Coral < 16.7 and Sand > Algae
dSC	Dominant sand with coral	50 < Sand < 66 and Coral > Algae OR Coral < 50 and Sand < 50 and Algae < 16.7 and Sand > Coral
CAS	Mixed coral/sand/algae	16.7 < Coral < 50 and 16.7 < Algae < 50 and 16.7 < Sand < 50
UC	Unclassified	

Table 3
Habitat area differences between 2009 and 2015 estimated for the Saint-Gilles coral reef unit. Absolute and relative values represent area increase rate (positive value) or decrease rate (negative values).

Coral reef habitat classes	Habitat area differences between 2009 and 2015 (ha)	Habitat area differences between 2009 and 2015 (%)
Coral	−5.4724	−28.24
Dominant coral with algae	−4.1932	−39.24
Dominant algae with coral	1.6605	+15.32
Algae	−1.2123	−0.95
Dominant algae with sand	12.0564	+78.43
Dominant sand with algae	3.2377	+28.50
Sand	−7.4056	−18.99
Sparse seagrass bed	0.0134	+3.70
Dense seagrass bed	0.4990	+57.64
Mixed coral/sand/algae	1.8052	+136.04
Dominant coral with sand	−0.2126	−58.33
Dominant sand with coral	0.0152	+9.71

each endmember. Two physical constraints were imposed on seabed-type retrieval: positive abundance and sum-to-one constraints.

2.3.4. Coral cover and coral to algae index estimation

In the present study, the coral to algae index derived from hyperspectral images (HCAI), calculated as the ratio of coral cover to the sum of coral and algae covers, is proposed as a proxy of coral reef health. This HCAI is developed after the "classical" coral to algae index (live coral cover over potentially available substrate) that is recognized by the local Reunion Island experts as a reef environmental quality indicator contributing to WFD implementation (Le Goff et al., 2012). Indeed, live coral cover is considered to be the most effective indicator of coral reef health (Huang et al, 2018). Earlier, Holden and Ledrew (2001) also indicated that although the health of coral reef ecosystem can be evaluated by different proxies, the only remotely detectable means of evaluation is through the presence of bleached or algae-covered coral because of the change in spectral reflectance in the visible wavelengths that are able to penetrate the water column (Holden and Ledrew, 2001).

2.3.5. Coral reef habitat mapping

Calculated cover rates of seabed components were used to produce a classified image from each of the two hyperspectral surveys (2009 and 2015). Thirteen habitat classes, combinations of cover rates of the four main benthic types as shown in Table 2, were considered to produce the coral reef habitat classification maps. The definition of these classes was based on the following principles:

(i) Seagrass are almost never mixed with coral at the pixel scale; this seabed habitat was first classified using its estimated cover rate with two classes "dense seagrass" beds and "sparse seagrass" beds.
(ii) Coral, algae and sand can be mixed in different proportions. Classes thresholds were set according to their respective proportions, from single dominant coral, algae, or sand habitats to coral/algae/sand mixtures.
(iii) Habitat maps and habitat areas were realized using ArcGIS software.

2.4. Spatial heterogeneity assessment

To limit the impact of the data geometric accuracy on the evaluation of the changes, a spatial filter was applied before performing change detection (Coppin et al., 2004). An appropriate window size was firstly defined to allow data smoothing without alteration of coral reef spatial distribution. We thus retrieved spatial heterogeneity characteristics to assess the impact of increasing the window size using geostatistical methods (Garrigues et al., 2006) with ISATIS software. Spatial variability was assessed based on sill values of variogram models fitted to coral cover experimental variograms.

We explicitly quantified the loss of spatial variability at different spatial resolution levels (i.e. 2 m, 5 m, 8 m, 10 m 20 m and 50 m) compared to the spatial variability at the initial fine resolution of 0.40 m. Cover maps generated at different lower spatial resolutions were obtained by averaging coral cover values over the number of pixels corresponding to the new defined resolutions.

2.5. Change detection quantification and mapping

Different approaches were used for the diachronic analyses, depending on the evaluated metric. These approaches were applied using the ArcGIS tool to estimate and map topography, coral cover and coral to algae index changes as detailed below.

2.5.1. Changes in digital elevation model

The digital elevation model (DEM) difference was produced based on a "pixel to pixel" approach. To our knowledge, no standard has been used to determine the areas where significant changes have occurred. A somewhat arbitrary threshold of one standard deviation around the mean was used to differentiate between change and no-change areas. Erosion or accretion were then considered as statistically significant when both limits of the standard deviation confidence interval were negative or positive, respectively. Spatial uncertainty related to the geometry of images was taken into account using a convolution filter (a

sliding average in a pixel-centered matrix) before computing image differences. The appropriate size of the filter window was determined by geostatistical analysis and set to 10 × 10 m (see Section 3.4 and Appendix C).

2.5.2. Coral cover and coral to algae index evolution

Coral cover evolution between 2009 and 2015 was also assessed with a "pixel to pixel" comparison approach, and the distribution of coral cover evolution was subsequently mapped. We carried out the change analysis only on the "coral entities" (CEs), thus using only pixels that could be assigned to corals: pixels exhibiting at least 30% of live coral, in order to ensure the inclusion of all types of live coral colonies (Fig. 3A).

Regarding the Hyperspectral Coral to Algae Index, analysis of changes was performed using an "aggregation approach" rather than working on individual pixels as for coral cover. The aggregation approach consisted in splitting the whole reef flat into rectangular polygons perpendicular to the coastline, where we calculated the mean of all the HCAI pixel values found in a given rectangle. We used 20 m width rectangles extending from the beach to the reef crest (400–500 m long) as shown in Fig. 3A.

2.5.3. Rubble tongue displacement

We assessed the change in each identified geomorphic coral structure on this fringing coral reef flat between 2003 and 2015 using high-spatial-resolution Pleiades satellite images, aerial photographies and high-resolution hyperspectral sensors. Four main rubble tongues (RT1 to RT4) were identified in Saint-Gilles reef flat unit. They were delineated manually based on visual image interpretation (Fig. 3B), after precise image-to-image co-registration with ENVI software (2015 as reference and mean RMS error < 0.4 m). Distances of displacement were then measured between consecutive dates using the ArcGIS tool.

3. Results

3.1. Coral cover

Field observations from 2015 field survey were used to validate estimated coral cover values from hyperspectral image processing as shown in Fig. 4A. There is a clear positive correlation (p-value < 0.001) with an adjusted coefficient of determination of 0.72 between coral cover observed in the field and that derived from image. Less significant correlation (Adjusted $R^2 = 0.51$, p-value = 0.04) was recorded between HCAI estimated by our image processing method and that observed *in situ* by the GCRMN (Fig. 4B) using lower number of samples.

The spatial heterogeneity in coral cover estimated from variogram analysis is shown in Appendix D. The site-fitted variogram model was approximated using two structures, both expressed as an exponential elementary variogram model with respectively ranges of 7 and 70 m and sills of 0.026 and 0.017. Variogram changes as a function of spatial resolution describe the effects of data regularization on the spatial heterogeneity components. The decrease in spatial variability with decreasing spatial resolution is characterized by a drop in the sill from 0.043 to 0.0059 for the 0.4 m and 50 m resolutions, respectively. The variograms have similar shapes and detect the same length scales from the initial resolution of 0.40 m to 10 m, but the first structure was no longer detectable by the variogram at coarser spatial resolutions (> 10 m). This analysis suggests that the resolution suitable to capture coral spatial heterogeneity must be around 8–10 m at the most.

Fig. 5A–B shows the changes between 2009 and 2015, from the variation of the CEs cover estimated from hyperspectral image processing. The values vary continuously between 0% and 100%, allowing a progressive view of coral colonization at the scale of the entire reef unit (Fig. 5A). The reef experienced high coral losses (in red) and coral gains (in blue) between 2009 and 2015 (Fig. 5B).

Coral cover increased up to 70% in some areas during the considered time frame, primarily in the southern "Trou d'Eau" sector in the La Saline sub-unit. Some important regressions (> 50%) were located in the center of the reef between the sanctuary zones, in particular just near south of Ermitage Pass (Fig. 5B).

3.2. Coral to algae index

The HCAI map (Fig. 5C) shows coral to algae index classified from low values (< 10%) to high values (> 70%). Depending on the area, reef changes between 2009 and 2015 showed different patterns. Aggregated HCAI differential distributions are in line with results obtained for CEs with a gain of 70% at the Trou d'Eau sanctuary area and a loss (> 25%) near Ermitage Pass (Fig. 5D).

Comparison with GCRMN field coral to algae index measurements shows a positive correlation with a coefficient of determination of 0.59 (Fig. 4B). These results are also in line with the *in situ* observations carried out through GCRMN protocol (Appendix D). The Toboggan station north of Ermitage Pass experienced an overall decrease in coral cover during the 2009–2015 period, while algal cover reached 75% of benthic cover in 2011. On the other hand, the Planch'Alizés station experienced an overall increase in coral cover and a decrease in algal cover between 2009 and 2015, particularly at the end of this period.

3.3. Coral reef habitats

The final coral reef habitat classification is shown in Fig. 6. The produced map includes 13 habitat classes representing the main reef substrates and benthic covers determined according to the criteria defined in Table 2.

The habitat maps show a heterogeneous distribution with homogeneous areas and habitat mosaics of the main habitat components (coral, seagrass, algae, and sand). Algal turf dominates in the reef flat area, up to the wave breaking zone (white masked for processing) next to the reef crest.

Image pairs reveal significant variation between 2009 and 2015, with different habitat types and at multiple locations of the reef (Fig. 6). In the narrow fringing reef of the northern part of the Saint-Gilles reef, the back reef (which is almost non-existent) was replaced either by a reef flat directly attached to the coast or by seagrass beds. The differences between the two images suggest that these types of habitat have progressed in this north sub-unit of Saint-Gilles reef (Fig. 6A1 and A2). A loss of seagrass beds occurred at the Ermitage center sub-unit with scattered patches, both dense and sparse (Fig. 6B1 and B2). Seagrasses are absent in the La Saline south sub-unit (Fig. 6C). The Ermitage sub-unit also experienced a loss of coral communities (Fig. 6B1 and B2), whereas the southern La Saline sub-unit showed a progression in coral communities near the restricted access sanctuary zone of the marine reserve (Fig. 6C1 and C2).

The habitat area comparison between 2009 and 2015 (Table 3) shows an overall progression in algal turf on sand, i.e. the "Dominant algae and sand" class increased by 78% and sand decreased by 19%. Coral areas showed a clear regression of 28.2% and 39.2% for the "Coral" and "Dominant coral with algae" classes respectively, at the expense of progression in the "Algae" classes (with a progression of 15.3% for the "Dominant algae with coral" class).

3.4. Digital elevation model

Bathymetry was directly derived from hyperspectral image processing. Fig. 7A shows the result obtained from the 2015 image. The maximum estimated depth is 1.5 m.

This bathymetry was validated by comparing the hyperspectral retrieval with Lidar data acquired in the same year (2009). The distribution of depth difference shows a clear correlation ($R^2 = 0.93$) between Lidar and hyperspectral estimated bathymetry. The mean

difference was estimated at −0.02 m with a standard deviation of 0.46 m.

The differential bathymetric map calculated between 2009 and 2015 DEMs varies from −0.99 m to 0.94 m (Fig. 7B). DEM difference classification underlines some geomorphological changes with erosion, accretion and unchanged areas (Fig. 7C). A sand/rubble bank displacement (1) was easily identified in the northwestern part of the reef flat as well as a sediment accumulation near Ermitage Pass (2) and a rubble tongue structure (3). Erosion mainly occurred close to the reef crest and accretion essentially close to the shoreline.

3.5. Rubble tongue displacement

Fig. 8 shows the outlines of the four rubble tongues obtained by photo-interpretation of the aerial and satellite images used for coral rubble tongue evolution. All studied tongues progressed between 2003 and 2015 and propagated towards the back reef at the expense of the existing live coral. However, RT01 and RT03 show a relatively narrow pointed shape, whereas RT02 and RT04 share a wider irregular shape.

Cumulative displacement was measured for each rubble tongue using the 2003 shape as a baseline. Displacement was measured with respect to both the outer reef side (ORS) and the back reef side (BRS) limits. Rubble tongue displacements, as well as a timeline of major weather events, are shown in Fig. 8. On average, the four RTs spread towards the back-reef by 8.38 ± 2.5 $m.y^{-1}$; however, RT displacement occurred at different rates. For RT01 and RT03, the rate of RT spreading was relatively fast and constant (average of 10.5 $m.y^{-1}$) while RT02 and RT04 showed a lower mean spread rate of 6.3 $m.y^{-1}$ between 2003 and 2017.

The BRS limits did not, or only very slightly, change during the studied period. However, the external live coral belt limits (ORS) progressed significantly towards the back reef. RT progression was continuous between 2003 and 2017 with a greater increase starting from 2009 but appeared to slow down after 2014. The difference between the ORS and BRS limits indicates the living coral belt width. The four RTs showed the same pattern of change, with 93% of the original live coral belt width being lost over a period of 14 years.

The topographic profiles of RT01 obtained from 2009 and 2015 DEMs hyperspectral images revealed important changes essentially distributed from 30 m to 150 m from the drawn profile origin (Fig. 9C). The 2015 topographic profile of RT01 shows a relative homogenization of depth along the transect line. The strong slope at 75 m in the 2009 profile indicates the RT limit and the interface between rubble spits and living coral colonies (Fig. 9A). These colonies are primarily composed of branching corals *Acropora muricata* (Fig. 9.3) that are well represented in the 2009 depth profile (75–170 m) where the topography displays succinct spatial variations characterized by these coral colonies. *In situ* observations confirm that the apical part of RT01 is composed mainly of rubble and broken coral fragments close to and surrounding living coral colonies (Fig. 9.2), whereas the downstream part of the RT01 is composed mainly of smooth, finger-like rubbles (Fig. 9.1).

4. Discussion

4.1. Changes in Reunion Island coral reef flat habitats

Changes in benthic habitats of the coral reefs have been investigated at the multiple decade scale (Ampou et al., 2018; Scopélitis et al., 2009). This study highlights a spatial approach based on multispectral and hyperspectral image analysis to detect benthic changes in a heterogeneous shallow coral reef flat of Reunion Island in the South-West Indian Ocean. Between 2009 and 2015, percent living coral varied significantly, demonstrating important coral regressions (> 50%) in some parts of the reef in particular close by the south of Ermitage Pass.

A coral reef habitat map was produced based on estimated benthic cover rates using an unmixing method applied to hyperspectral water column-corrected images. We defined 13 habitat classes based on field benthic identification. Image pixels were classified according to their respective proportions, from a single dominant component (seagrass, coral, algae, or sand) habitat to coral/algae/sand mixtures. Fewer classes than Scopélitis et al. (2009) were used (i.e. 15 classes), which required a handmade map associated with qualitative observations and semi-quantitative descriptions of benthic communities. On the other hand, Palandro et al. (2008) only used four benthic classes derived from automatic image classification, revealing inconsistencies when the spatial distribution of the different classes varies too abruptly to be realistic. Our classification scheme, based on the proportions of the benthic components within each pixel, demonstrates a clear and easy pathway to objectively and rigorously define benthic habitat classes. Presence of both qualitative and quantitative descriptions rather than an arbitrary class labeling definition ensure an unambiguous interpretability of mapped habitats. However, obtained classification is restricted in some particular sub-classes distinction, with for instance, crustose coralline algae, turf algae and the different fleshy macroalgae categories within the algae super-class that are not discriminated. This may under or overestimate the real weight of these distinctive benthic communities that play an important role in the ecology of coral reefs. Besides, implemented image processing does not take into account spectral variability that exists even for the same species (Fig. 11). Further analyses are required to evaluate its impact on habitat classification performance, mainly for mixed areas.

As illustrated by the classification map (Fig. 6), coral habitat distribution varied significantly between 2009 and 2015. We highlighted substantial losses of live coral at the Ermitage sub-unit (Fig. 6B), although this habitat class seems to be progressing in its southern portion (Fig. 6C). Semple (1997) indicated that the coral communities of the fringing reef complex at Saint-Gilles are clearly subjected to degradation, likely due to water enrichment and extensive submarine groundwater discharge. No sign of coral degradation has been reported before 1983 (Guillaume et al., 1983) in this region. In the early 1970s, Faure (1982) reported 50% of coral cover on the outer compact reef flat and 50% of cover on the inner reef flat zone. Living coral represented only 11% of the substratum on the reef flat in 1993, with only 1.5% on outer compact reef flat and 3% on the back reef (Naim, 1993). Tourrand et al. (2013) documented temporal and spatial trends of benthic communities over a 22-year period (1987–2009), on the largest reef flat in RI, Saint-Gilles La Saline and proposed possible explanations of major coral cover changes such as bleaching events, cyclones, extreme tides and eutrophication.

As mentioned by Semple (1997), few differences were detected in the back-reef zone except a modification in seagrass distribution more or less fragmented from north to south. The ones from the northern end of the reef appear to be in extension, while the Ermitage sub-units appear to be regressing. Seagrass bed pattern analysis over 65 years by Cuvillier et al. (2017) at Saint-Gilles reveals that physical factors (austral winter swell events, cyclones) have a major impact, although biotic factors such as herbivory also influence the structural shape of seagrass beds. Regarding algae, our results highlighted a clear progression of algal turf cover between 2009 and 2015. Simultaneously, a clear regression of 28.2% and 39.2% occurred respectively for the “Coral” and “Dominant coral with algae” habitat classes while the “Algae” habitat class progressed, along with the 15.3% progression of the “Dominant algae with coral” habitat class. However, the Algae habitat in the RI reef is mainly made up of algal turf, with microscopic and very diffuse cover that can vary at the temporal scale of only a few weeks. Over the sandy seabed, microphytobenthos may also contribute to the hyperspectral signal. The diffuse nature of algae and sand make their cover rates very difficult to accurately assess using remote sensing imagery, particularly at the limits of the linear mixing model.

4.1.1. Coral cover and Hyperspectral Coral to Algae Index (HCAI) evolution

Using hyperspectral imaging, we were able to assess quantitatively coral reef health through HCAI, expressed as the ratio of living coral to the sum of coral and algal covers. There was a significant correlation between coral cover estimated in the field and derived from images, with an adjust R^2 of 0.72. This value is of the same order of magnitude as that obtained by Huang et al. (2018) and much higher than the coefficient reported in the study carried out by Joyce et al. (2013). Such a result sustains the effectiveness and feasibility of the used method. It is however important, in estimating the changes, that the same method is used to process the multidate data to ensure that the detected change does not potentially reflect the bias associated with the use of different processing method. In gradually and continuously spatially changing environments, uncertainties and subjectivity of boundaries imposed by conventional classification methods (Andréfouët, 2012) can be avoided using continuous values of coral cover and HCAI indexes assessed by hyperspectral data unmixing. Coral cover and HCAI were not homogeneous over the Saint-Gilles reef unit. Although these indices improved between 2009 and 2015 in the southern La Saline sub-unit, we noted substantial coral degradation around Ermitage Pass, including at the Toboggan station despite its proximity to the MPA sanctuary zone. Bigot et al. (2016) also demonstrated that the establishment of an MPA sanctuary zone since 2007 has not improved the temporal dynamics of coral cover. External factors linked to a chronic increase in the sources of diffuse pollution from adjacent watersheds that reach Ermitage Pass or to high nutrient inputs via rivers and submarine groundwater discharge are likely to be the main factors explaining these degradations (Chazottes et al., 2002). The La Saline fringing reef ecosystem was also moderately to highly contaminated with hydrocarbons (Guigue et al., 2015). The sanctuary zones represent only 5% of the RNMR MPAs, which is probably insufficient to favor ecological processes that help restore good health status. The trends highlighted in the present study are also supported by the difference estimated per unit of aggregation (Fig. 5D), which integrates the entire reef flat between the coastline and the seaward reef crest and shows the changes in the average value of HCAI index along the coast. It may also be a useful management tool to facilitate the identification of spatial and temporal changes.

It remains difficult to formally determine the exact origin of changes, especially because detected changes do not display the same pattern across the entire Saint-Gilles reef. In some coral reef ecosystems that have experienced disturbance and erosion of resilience, a phase shift has been observed, which is most often reflected in the non-temporary transition from a coral-dominated ecosystem to an algae-dominant ecosystem (Bellwood et al., 2006), in particular when nutrient outputs increase, and herbivore grazing pressure decreases (Mumby et al., 2007). Some RI reef areas appear to be undergoing this phase shift, which can have dramatic consequences in terms of maintaining reef function (Bigot et al., 2016). Low tide exposure events can potentially contribute significantly to erosion, resulting in high coral mortality (Baker et al., 2008). In general, vertical coral growth stops at the low tide level. Corals cannot tolerate prolonged exposure, except for certain species such as *Porites* spp. which can resist desiccation by secreting mucus. This probably explains why the southern Saint-Gilles coral reefs are healthier with *Porites* corals more frequent in this area. Strong austral swell events as well as tropical hurricanes affect geomorphological structures and ecological functions of coral reef ecosystems (Massel and Done, 1993). During the present study, recurrent strong swell events (6 m in 2013 and 2014) occurred at the Ermitage and La Saline sub-units.

4.1.2. Modifications in coral reef topography

The ability to detect change in a geomorphological parameter is a key output for ecosystem monitoring (Coppin et al., 2004; Garcia et al., 2014). Our results show that hyperspectral image processing can accurately retrieve consistent depths despite uncertainties associated with topographic complexity, geometric precision and processing methods.

High spatial resolution of 0.4 m appears to be well adapted to the spatial heterogeneity of RI coral reefs, given the spatial consistency of several geomorphological features detected in this area. The differential bathymetric map (Fig. 7), calculated from the 2009 and 2015 DEMs, captured temporal changes occurring in the three-dimensional structure that characterizes these shallow areas. Movements of the two sand/rubble banks across the reef flat northwest of Ermitage Pass indicate that detected changes are most likely related to wave action, and more specifically to wave-induced currents rather than tidal forcing. The differential bathymetry also revealed changes due to sediment movements near the mouth of Ermitage Pass, presumably due to high sediment deposition. Similar sediment movements were highlighted by Garcia et al. (2014) with changes in depth due to sediment reworking near the mouth of the Wooramel River (Western Australia). Due to the two modes of sand transport depending on weather conditions, Cordier (2007) established that, in Reunion back reef areas, all types of sand, from fine to coarse sand, are transported.

4.1.3. Changes in coral rubble features

Evidence of structural coral reef loss has been documented in previous studies (Lewis, 2002; Shannon et al., 2013). In RI main rubble tongues are essentially composed of coral fragments with significant loss of reef structural complexity and heterogeneity. All prospected rubble tongues progressed shoreward between 2003 and 2015. The mean spread rate occurred at an alarming speed of 8.4 ± 2.5 $m.y^{-1}$, with a maximum value of 10.5 $m.y^{-1}$. On One Tree Reef (southern Great Barrier Reef, Australia), the greatest rate of displacement of 12.3 $m.y^{-1}$ was recorded between 1978 and 1980 (Shannon et al., 2013).

Regarding the driving process, rubble tongue formation has been addressed in previous studies with conceptual models. Etienne and Terry (2012) described T-shape tongues of coral rubble formed on Taveuni Island (Fiji) reef flats. They suggested that this structure may reflect the effect of wave refraction on loose sediment during cyclonic events. In fact, branching corals in the upper part of the outer reef are severely abraded so that where the outer reef slope is relatively gentle, coral rubble is removed and redistributed over the reef flat (Harmelin-Vivien and Laboute, 1986). Shannon et al. (2013) formulated the hypothesis that the location of these structures is related to the outer reef morphology of large spurs and grooves that lead waves to focus their energy and hence transport larger rubble sediments forming a spit, particularly when they are formed following major storm events such as tropical hurricanes. In the present study, rubble tongues spread continuously during the study period, even in the absence of extreme events between 2008 and 2013, and no particular outer reef spurs-and-grooves pattern was specifically identified in front of the rubble tongues.

Bayliss-Smith (1988) observed that strong storm waves are the only marine process capable of displacing large-volume coral rubble ridges in a short time. However, the gradient of live and dead coral content along a cross-shore transect over the rubble tongue, with broken coral in the apical part (Fig. 9A), suggests mainly a local contribution to rubble tongue formation. Branching corals have greater potential for destruction (hence sediment delivery) than massive or short-branching

colonies (Harmelin-Vivien and Laboute, 1986). We therefore suppose that particular local hydrodynamic conditions have driven rapid coral degradation and the development of rubble tongues. The continuous advancement of RT could also be related to *Acropora muricata* mortality due to anthropogenic stressors. Cordier (2007) also established that under the effect of currents, particles are transported along an axis generally perpendicular to the coast, in the direction of the rubble tongue progression. As it was well established by changes in the depth profile, reef rubble tongues typically showed a landward edge thickness of around 0.5 m, similar to the value measured by Etienne and Terry (2012) in the Taveuni Island (Fiji).

Furthermore, the rubble tongues exhibited different shapes: pointed shape with faster progression for RT01 and RT03, (especially between 2012 and 2015), and wider shape with slower progression for RT02 and RT04. The complex interaction between rubble supply, wave energy direction and outer reef morphology is the dominant control on the shape and evolution of rubble flats and rubble spits (Shannon et al., 2013). Refraction tends to foster the focusing of wave fronts towards a focal point located on the reef flat (Mandlier and Kench, 2012).

4.1.4. Coherence between monitoring scales

The comparison of the results obtained at the GCRMN field stations and those obtained from hyperspectral images does not appear to show any inconsistencies, although these two approaches differ fundamentally in many aspects, namely: (i) their resolution (linear transect *versus* areal large-scale coverage), (ii) the parameters measured (community structure *versus* habitat), and (iii) the precision of the information obtained (*in situ* observed *versus* remotely estimated). The “live coral cover” and the HCAI showed similar trends. Therefore, for RI reef sites, the GCRMN and hyperspectral image approaches provide comparable and complementary measurements of reef status and benthic dynamics, although the information was acquired at different spatial and ecological scales. It should however be pointed out that the GCRMN positioning of transects is constrained by the surrounding reef morphology. Therefore, these transects may not represent the whole reef flat, particularly at some very heterogeneous stations such as Planch’Alizés on the La Saline sub-unit.

It should also be highlighted that line transects, initially designed for global coral reef health status monitoring, were obviously positioned in high coral cover areas. Therefore, extrapolating results beyond the line transects would introduce significant bias. As was suggested by Palandro et al. (2008), local and high-frequency measurements of loss (coral cover, benthic community structure) — as conducted by GCRMN — can be supplemented with broader spatial measurements of habitat dynamics and fragmentation through low-frequency spatial monitoring. Spatial approach is also more suitable for describing natural patterns emerging from a range of gradients (Austin, 2007).

4.1.5. Issues and future research

Our study of the main RI fringing reef confirms the usefulness of hyperspectral imaging to spatially characterize the health status of coral reefs and to monitor the temporal changes in shallow water coral habitats. Nevertheless, future avenues of research can help enhance the effectiveness of the methodology applied here. Only two dates in a six-year period were used for this study. As suggested by Scopélitis et al. (2009), more frequent surveys depicting the distribution and spatial heterogeneity of coral communities over time may provide key information on coral resilience, diversity, and dynamics. Recommendations call for image acquisition frequency every four years if no particular events occur, with additional surveys immediately after disturbances such as hurricanes. Moreover, the methods used are limited to the shallow reef flat area with depth not exceeding 2 m. The recent methodological work carried out on Reunion Island on small test zones showed that it is possible to estimate the bathymetry with high confidence to about 20 m and to detect the main seabed types up to 10 m (Petit et al., 2017). Optimizing these algorithms to operationally process the data from all RI reefs would be of great value. Although the process of change detection, as implemented in this study, provides useful results, there are limitations related to image characteristics including differences in the sensors and spectral resolutions used, as well as in atmospheric correction pre-processing. Future studies should follow the main recommendations to minimize errors and biases in the process of change detection (Pathak, 2014). Relating changes in bathymetry to factors such as accretion/erosion implies removing the tidal contribution to the retrieved water column depth. For this study, depth was estimated using a single value to bring back estimated water column height to the hydrographical reference. As suggested by Garcia et al. (2014), tidal modeling would be necessary to interpolate (either linearly or non-linearly) the tide correction offsets for the different regions to generate a homogeneous tide-corrected bathymetry image. In addition, further investigations are needed to better estimate uncertainty and investigate whether other thresholds applied to differences between images would provide better results (Vanderstraete et al., 2006).

5. Conclusion

Reunion Island young reef ecosystems, exposed to various human-driven and natural pressures, highlight a challenge in the understanding and management of its benthic communities, and in particular the “coral-macroalgae” dynamics. This study describes the methodological approaches used to locate and quantify the changes that took place in the Saint-Gilles reef flat over a six-year period. In contrast with field surveys of coral reef status, we favored here a quantitative spatial approach to evaluate changes based mainly on hyperspectral images to extract both depth and seabed information. To our knowledge, this is the first time that Reunion Island coral reef geomorphology and habitats as well as coral reef health status with HCAI have been mapped to provide trends across the whole Saint-Gilles reef flat, using automatic methods in conjunction with a field point-based survey (i.e. GCRMN). This global approach makes it possible to compare different sites objectively, by evaluating several metrics on a scale suitable for conservation planning and resource assessment. Through a diachronic analysis, the present study confirms and illustrates the value of hyperspectral technology for assessing changes (gains and losses) in coral cover and HCAI as well as for reef flat geomorphology, opening up new perspectives for operational monitoring at broader scale. By analyzing changes in the types of main seabed cover and bathymetry taking into account uncertainty, we clearly observed significant changes in the Reunion Island reef flat over a period of six years. These changes mostly involved algal and coral cover, although changes in the extent of other habitat component types such as seagrass beds, were also recorded. Caution should be taken, however, in recognizing the potential errors and precision limits inherent to hyperspectral image datasets and their pre-processing. Also the possibilities offered by the spectral unmixing processing revealed intra-pixel information that cannot be obtained using conventional classification tools. In mosaic and highly heterogeneous environments, such as the Reunion Island reefs, this spatial approach proved to be valuable. Although this study raised issues related to data and processing limitations, it also provided useful results and identified areas for improvement, to extract more accurate information from hyperspectral data. Further research is needed to better explain the observed changes and to establish the links to their main drivers.

Acknowledgements

This work was supported by (i) the SPECTRHABENT-OI project, funded by the Prefecture and the Directorate for Environment, Development and Housing (DEAL) of Reunion Island, the French Southern and Antarctic Lands (TAAF), the French Marine Protected Area Agency (AAMP) and Ifremer and (ii) the HYSCORES project, funded by the Reunion Water Office, Ifremer, the University of Western Brittany and the Tosca program (Hypercoral project).

Access to Pleiades images was granted by the CNES programs RTU, ISIS and Kalideos Reunion.

We are very grateful to all those who participated in the airborne and field surveys. The fieldwork could not have been completed without valuable contributions from the Reunion Marine Reserve (RNMR).

We wish to thank Carolyn Engel-Gautier, Amelia Curd and Flavia Nunes for reviewing the English.

We are very grateful to Ronan Le Goff, for believing in the interest of the hyperspectral for environmental monitoring, and to Pascal Talec from DEAL Reunion, for his constance in strengthening the link between scientists and managers.

Appendices

Appendix A. Multi-temporal image sub-sets corresponding of the four studied rubble tongues (RT1, RT2, RT3, RT4) between 2003 and 2017.

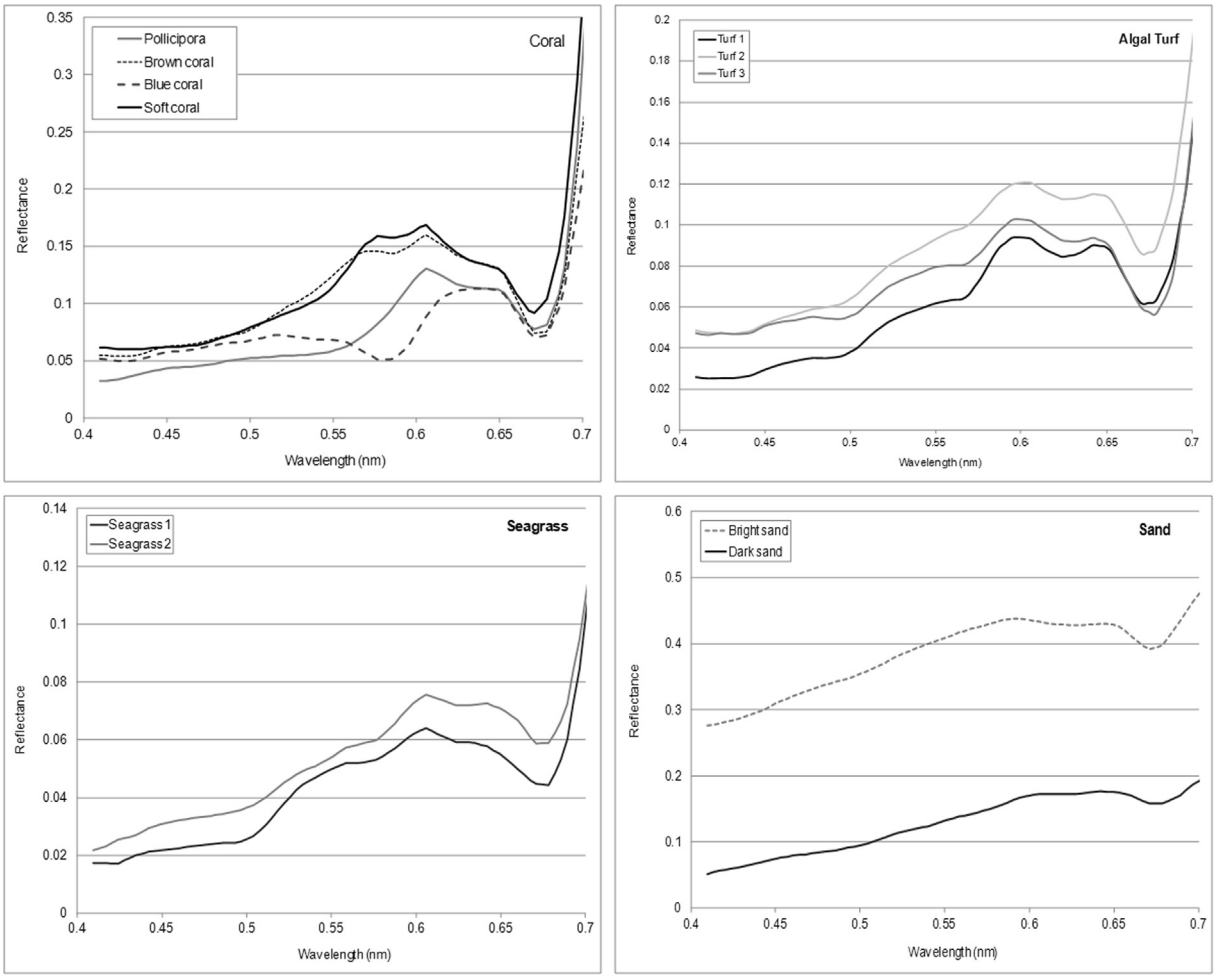

Appendix B. Spectral variability of the main Reunion coral reef seabed types: corals, algal turf, seagrass, and sand.

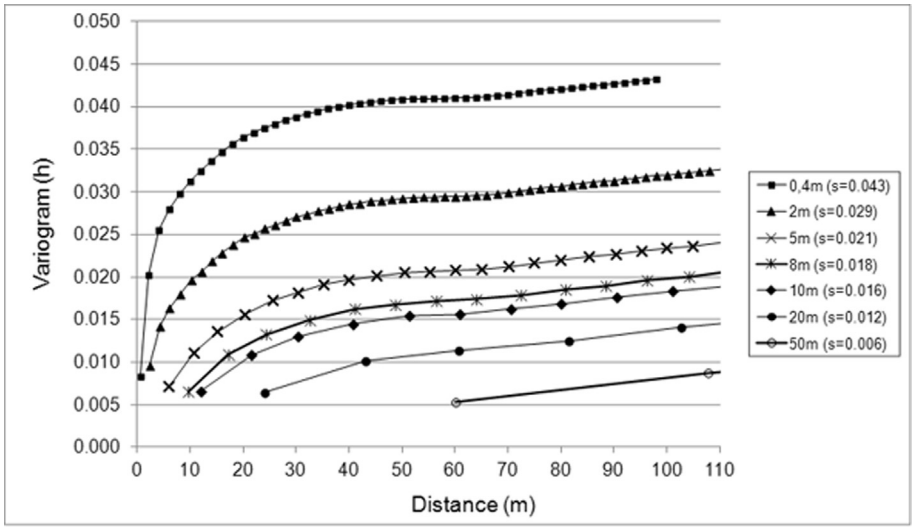

Appendix C. Effect of decreasing the image spatial resolution on the coral cover variogram shape and sill(s).

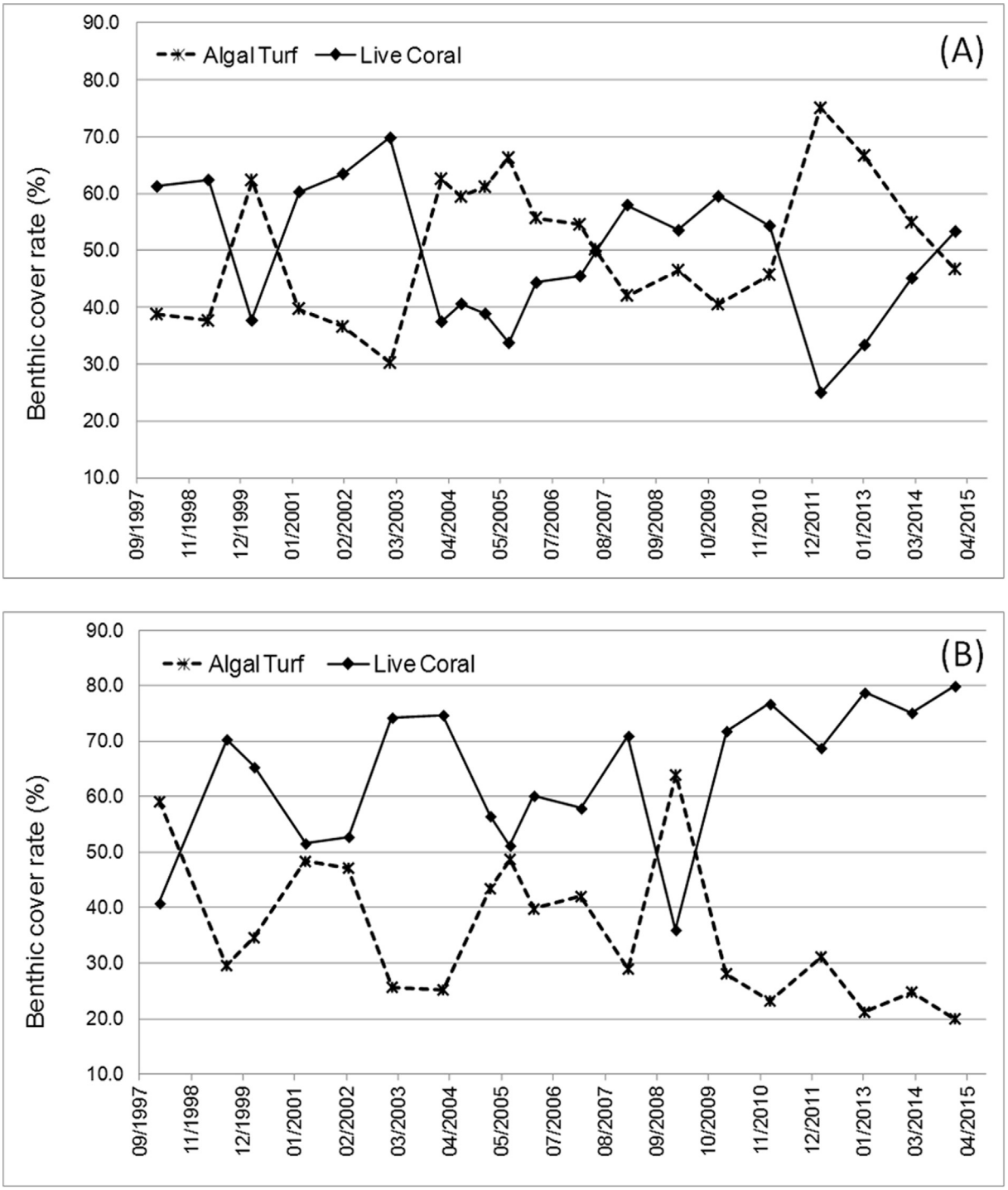

Appendix D. Changes in coral and algal turf cover monitored as part of the Global Coral Monitoring program for the Toboggan (A) and Planch'Alizés (B) stations.

References

Allemand, D., Tambutté, É., Zoccola, D., Tambutté, S., 2011. Coral calcification, cells to reefs. In: Coral Reefs: An Ecosystem in Transition. Springer Netherlands, Dordrecht, pp. 119–150.

Ampou, E.E., Ouillon, S., Iovan, C., Andréfouët, S., 2018. Change detection of Bunaken Island coral reefs using 15 years of very high resolution satellite images: a kaleidoscope of habitat trajectories. Mar. Pollut. Bull. 131, 83–95. https://doi.org/10.1016/j.marpolbul.2017.10.067.

Andréfouët S., 2012. Mozambique Channel Coral Reef Habitat Mapping. Report to Collecte Localisation Satellites. IRD, Nouméa, January 2012. p. 56.

Andréfouët, S., Muller-Karger, F.E., Hochberg, E.J., Hu, C., Carder, K.L., 2001. Change detection in shallow coral reef environments using Landsat 7 ETM+ data. Remote Sens. Environ. 78, 150–162. https://doi.org/10.1016/S0034-4257(01)00256-5.

Andréfouët, S., Payri, C., Hochberg, E.J., Hu, C., Atkinson, M.J., Muller-Karger, F.E., 2004. Use of in situ and airborne reflectance for scaling-up spectral discrimination of coral reef macroalgae from species to communities. Mar. Ecol. Prog. Ser. 283, 161–177. https://doi.org/10.3354/meps283161.

Austin, M.P., 2007. Species distribution models and ecological theory: a critical assessment and some possible new approaches. Ecol. Model. 200, 1–19. https://doi.org/10.1016/j.ecolmodel.2006.07.005.

Baker, A.C., Glynn, P.W., Riegl, B., 2008. Climate change and coral reef bleaching: an ecological assessment of long-term impacts, recovery trends and future outlook. Estuar. Coast. Shelf Sci. 80, 435–471. https://doi.org/10.1016/j.ecss.2008.09.003.

Bayliss-Smith, T.P., 1988. The role of hurricanes in the development of reef islands, Ontong Java atoll, Solomon Islands. Geogr. J. 154, 377–391. https://doi.org/10.2307/634610.

Bellwood, D.R., Hughes, T.P., Folke, C., Nyström, M., 2004. Confronting the coral reef crisis. Nature 429, 827–833. https://doi.org/10.1038/nature02691.
Bellwood, D.R., Hughes, T.P., Hoey, A.S., 2006. Sleeping functional group drives coral-reef recovery. Curr. Biol. 16, 2434–2439. https://doi.org/10.1016/j.cub.2006.10.030.
Bigot, L., Bruggemann, H., Cadet, C., Cauvin, B., Chabanet, P., Durville, P., Guillaume, M., Mulochau, T., Penin, L., Tessie, E., Urbina, I., 2016. Point I du suivi de « l'effet réserve » sur les communautés ichtyologiques et benthiques récifales - Secteurs de St Gilles/La Saline et de Saint-Leu - Etat des lieux à 7 ans après la création de la Réserve Naturelle Nationale Marine de La Réunion. Rapport final. 59p + annexes.
Bioucas-Dias, J.M., Plaza, A., Dobigeon, N., Parente, M., Du, Q., Gader, P., Chanussot, J., 2012. Hyperspectral unmixing overview: geometrical, statistical, and sparse regression-based approaches. IEEE J. Sel. Top. Appl. Earth Obs. Remote Sens. https://doi.org/10.1109/JSTARS.2012.2194696.
Bozec, Y.-M., Mumby, P.J., 2014. Synergistic impacts of global warming on the resilience of coral reefs. 20130267 20130267. Philos. Trans. R. Soc. B Biol. Sci. 370. https://doi.org/10.1098/rstb.2013.0267.
Chabanet, P., Bigot, L., Naim, O., Garnier, R., Mayne-Picard, M., 2002. Coral reef monitoring at Reunion island (Western Indian Ocean). In: Proceedings of the 9th International Coral Reef Symposium in Bali, Indonesia, vol. 2, pp. 873–878.
Chazottes, V., Le Campion Alsumard, T., Peyrot-Clausade, M., Cuet, P., 2002. The effects of eutrophication-related alterations to coral reef communities on agents and rates of bioerosion (Reunion Island, Indian Ocean). Coral Reefs 21, 375–390. https://doi.org/10.1007/s00338-002-0259-0.
Coppin, P., Jonckheere, I., Nackaerts, K., Muys, B., Lambin, E., 2004. Digital change detection methods in ecosystem monitoring: a review. Int. J. Remote Sens. 25, 1565–1596. https://doi.org/10.1080/0143116031000101675.
Cordier, E., 2007. Processus physiques et sédimentaires en milieu récifal: application aux récifs frangeants de l'Hermitage/La Saline, Ile de La Réunion (Ph.D. thesis). Université de la Réunion, France. p. 150.
Cuvillier, A., Villeneuve, N., Cordier, E., Kolasinski, J., Maurel, L., Farnier, N., Frouin, P., 2017. Causes of seasonal and decadal variability in a tropical seagrass seascape (Reunion Island, south western Indian Ocean). Estuar. Coast. Shelf Sci. 184, 90–101. https://doi.org/10.1016/j.ecss.2016.10.046.
Done, T., Turak, E., Wakeford, M., DeVantier, L., McDonald, A., Fisk, D., 2007. Decadal changes in turbid-water coral communities at Pandora Reef: loss of resilience or too soon to tell? Coral Reefs 26, 789–805. https://doi.org/10.1007/s00338-007-0265-3.
Etienne, S., Terry, J.P., 2012. Coral boulders, gravel tongues and sand sheets: features of coastal accretion and sediment nourishment by Cyclone Tomas (March 2010) on Taveuni Island, Fiji. Geomorphology 175–176, 54–65. https://doi.org/10.1016/j.geomorph.2012.06.018.
Facon, M., Pinault, M., Obura, D., Pioch, S., Pothin, K., Bigot, L., Garnier, R., Quod, J.P., 2016. A comparative study of the accuracy and effectiveness of Line and Point Intercept Transect methods for coral reef monitoring in the southwestern Indian Ocean islands. Ecol. Ind. 60, 1045–1055. https://doi.org/10.1016/j.ecolind.2015.09.005.
Faure, G., 1982. Recherche sur les peuplements de Scleractinaires des récifs coralliens de l'Archipel des Masccareignes (Ocean Indien Occidental). (Ph.D. thesis). Université Aix-Marseille II, France. p. 206.
Ferrario, F., Beck, M.W., Storlazzi, C.D., Micheli, F., Shepard, C.C., Airoldi, L., 2014. The effectiveness of coral reefs for coastal hazard risk reduction and adaptation. Nat. Commun. 5, 3794. https://doi.org/10.1038/ncomms4794.
Garcia, R.A., Fearns, P.R.C.S., McKinna, L.I.W., 2014. Detecting trend and seasonal changes in bathymetry derived from HICO imagery: a case study of Shark Bay, Western Australia. Remote Sens. Environ. 147, 186–205. https://doi.org/10.1016/j.rse.2014.03.010.
Garcia, R.A., Lee, Z., Hochberg, E.J., 2018. Hyperspectral shallow-water remote sensing with an enhanced benthic classifier. Remote Sens. 10, 147. https://doi.org/10.3390/rs10010147.
Garrigues, S., Allard, D., Baret, F., Weiss, M., 2006. Quantifying spatial heterogeneity at the landscape scale using variogram models. Remote Sens. Environ. 103, 81–96. https://doi.org/10.1016/j.rse.2006.03.013.
Guannel, G., Arkema, K., Ruggiero, P., Verutes, G., 2016. The power of three: coral reefs, seagrasses and mangroves protect coastal regions and increase their resilience. PLoS One 11, e0158094. https://doi.org/10.1371/journal.pone.0158094.
Guigue, C., Bigot, L., Turquet, J., Tedetti, M., Ferretto, N., Goutx, M., Cuet, P., 2015. Hydrocarbons in a coral reef ecosystem subjected to anthropogenic pressures (La Réunion Island, Indian Ocean). Environ. Chem. 12, 350. https://doi.org/10.1071/EN14194.
Guillaume, M., Payri, C.E., Faure, G., 1983. Blatant Degradation of Coral Reefs at La Reunion Island (West Indian). Int. Soc. For Reef Studies Nice (Abstract).
Halpern, B.S., Selkoe, K.A., Micheli, F., Kappel, C.V., 2007. Evaluating and ranking the vulnerability of global marine ecosystems to anthropogenic threats. Conserv. Biol. 21, 1301–1315. https://doi.org/10.1111/j.1523-1739.2007.00752.x.
Harborne, A.R., Rogers, A., Bozec, Y.-M., Mumby, P.J., 2017. Multiple stressors and the functioning of coral reefs. Ann. Rev. Mar. Sci. 9, 445–468. https://doi.org/10.1146/annurev-marine-010816-060551.
Harmelin-Vivien, M.L., Laboute, P., 1986. Catastrophic impact of hurricanes on atoll outer reef slopes in the Tuamotu (French Polynesia). Coral Reefs 5, 55–62. https://doi.org/10.1007/BF00270353.
Hedley, J.D., Roelfsema, C.M., Chollett, I., Harborne, A.R., Heron, S.F., Weeks, S.J., Skirving, W.J., Strong, A.E., Mark Eakin, C., Christensen, T.R.L., Ticzon, V., Bejarano, S., Mumby, P.J., 2016. Remote sensing of coral reefs for monitoring and management: a review. Remote Sens. 8, 118. https://doi.org/10.3390/rs8020118.
Hochberg, E.J., Atkinson, M.J., 2000. Spectral discrimination of coral reef benthic communities. Coral Reefs 19, 164–171. https://doi.org/10.1007/s003380000087.
Holden, H., LeDrew, E., 1998. Spectral discrimination of healthy and non-healthy corals based on cluster analysis, principal components analysis, and derivative spectroscopy. Remote Sens. Environ. 65, 217–224. https://doi.org/10.1016/S0034-4257(98)00029-7.
Holden, H., LeDrew, E., 2001. Hyperspectral discrimination of healthy versus stressed corals using in situ reflectance. J. Coast. Res. 17, 850–858. https://doi.org/10.2307/4300244.
Huang, R., Yu, K., Wang, Y., Wang, W., Mu, L., Wang, J., 2018. Method to design a live coral cover sensitive index for multispectral satellite images. Opt. Express 26, A374–A397. https://doi.org/10.1364/OE.26.00A374.
Hughes, T.P., Barnes, M.L., Bellwood, D.R., Cinner, J.E., Cumming, G.S., Jackson, J.B.C., Kleypas, J., Van De Leemput, I.A., Lough, J.M., Morrison, T.H., Palumbi, S.R., Van Nes, E.H., Scheffer, M., 2017. Coral reefs in the Anthropocene. Nature 546, 82–90. https://doi.org/10.1038/nature22901.
Joyce, K.E., Phinn, S.R., Roelfsema, C.M., 2013. Live Coral cover index testing and application with hyperspectral airborne image data. Remote Sens. 5, 6116–6137. https://doi.org/10.3390/rs5116116.
Karpouzli, E., Malthus, T.J., Place, C.J., 2004. Hyperspectral discrimination of coral reef benthic communities in the western Caribbean. Coral Reefs 23, 141–151. https://doi.org/10.1007/s00338-003-0363-9.
Kobryn, H.T., Wouters, K., Beckley, L.E., Heege, T., 2013. Ningaloo reef: shallow marine habitats mapped using a hyperspectral sensor. PLoS One 8, e70105. https://doi.org/10.1371/journal.pone.0070105.
Lee, Z., Carder, K.L., Mobley, C.D., Steward, R.G., Patch, J.S., 1998. Hyperspectral remote sensing for shallow waters I A semianalytical model. Appl. Opt. 37, 6329–6338. https://doi.org/10.1364/AO.37.006329.
Le Goff, R., Ropert, M., Bajjouk, T., Bein, A., Cambert, H., Cebeillac, A., Cuet, P., Delacourt, C., Duval, M., Maurel, L., Mouquet, P., Nicet, J.B., Populus, J., Quod, J.P., Talec, P., Turquet, J., Vermenot, C., Zubia, M., 2012. Projet Bio indication à La Réunion. Contribution au développement d'indicateurs adaptés aux platiers récifaux de La Réunion. Rapport final 2012. p. 107. http://archimer.ifremer.fr/doc/00209/32022/.
Lewis, J.B., 2002. Evidence from aerial photography of structural loss of coral reefs at Barbados, West Indies. Coral Reefs 21, 49–56. https://doi.org/10.1007/s00338-001-0198-1.
Madin, J.S., Madin, E.M.P., 2015. The full extent of the global coral reef crisis. Conserv. Biol. 29, 1724–1726. https://doi.org/10.1111/cobi.12564.
Mandlier, P.G., Kench, P.S., 2012. Analytical modelling of wave refraction and convergence on coral reef platforms: implications for island formation and stability. Geomorphology 159–160, 84–92. https://doi.org/10.1016/j.geomorph.2012.03.007.
Massel, S.R., Done, T.J., 1993. Effects of cyclone waves on massive coral assemblages on the Great Barrier Reef: meteorology, hydrodynamics and demography. Coral Reefs 12, 153–166. https://doi.org/10.1007/BF00334475.
Mishra, D.R., Narumalani, S., Rundquist, D., Lawson, M., Perk, R., 2007. Enhancing the detection and classification of coral reef and associated benthic habitats: a hyperspectral remote sensing approach. J. Geophys. Res. Ocean. 112, C08014. https://doi.org/10.1029/2006JC003892.
Mumby, P.J., Hastings, A., Edwards, H.J., 2007. Thresholds and the resilience of Caribbean coral reefs. Nature 450, 98–101. https://doi.org/10.1038/nature06252.
Naim, O., 1993. Seasonal responses of a fringing reef community to eutrophication (Reunion Island, Western Indian Ocean). Mar. Ecol. Prog. Ser. 99, 137–151. https://doi.org/10.3354/meps099137.
Palandro, D.A., Andréfouët, S., Hu, C., Hallock, P., Müller-Karger, F.E., Dustan, P., Beaver, C.R., 2008. Quantification of two decades of shallow-water coral reef habitat decline in the Florida Keys National Marine Sanctuary using Landsat data (1984–2002). Remote Sens. Environ. 112, 3388–3399. https://doi.org/10.1016/j.rse.2008.02.015.
Pathak, S., 2014. New Change Detection Techniques to monitor land cover dynamics in mine environment. In: International Archives of the Photogrammetry, Remote Sensing and Spatial Information Sciences – ISPRS Archives. pp. 875–879. https://doi.org/10.5194/isprsarchives-XL-8-875-2014.
Perry, C.T., Spencer, T., Kench, P.S., 2008. Carbonate budgets and reef production states: a geomorphic perspective on the ecological phase-shift concept. Coral Reefs 27, 853–866. https://doi.org/10.1007/s00338-008-0418-z.
Petit, T., Bajjouk, T., Mouquet, P., Rochette, S., Vozel, B., Delacourt, C., 2017. Hyperspectral remote sensing of coral reefs by semi-analytical model inversion – Comparison of different inversion setups. Remote Sens. Environ. 190, 348–365. https://doi.org/10.1016/j.rse.2017.01.004.
Scopélitis, J., Andréfouët, S., Phinn, S., Chabanet, P., Naim, O., Tourrand, C., Done, T., 2009. Changes of coral communities over 35 years: integrating in situ and remote-sensing data on Saint-Leu Reef (la Réunion, Indian Ocean). Estuar. Coast. Shelf Sci. 84, 342–352. https://doi.org/10.1016/j.ecss.2009.04.030.
Semple, S., 1997. Algal growth on two sections of a fringing coral reef subject to different levels of eutrophication in Reunion Island. Oceanol. Acta 20, 851–861.

Shannon, A.M., Power, H.E., Webster, J.M., Vila-Concejo, A., 2013. Evolution of coral rubble deposits on a reef platform as detected by remote sensing. Remote Sens. 5, 1–18. https://doi.org/10.3390/rs5010001.

Spalding, M., Burke, L., Wood, S.A., Ashpole, J., Hutchison, J., Zu Ermgassen, P., 2017. Mapping the global value and distribution of coral reef tourism. Mar. Policy 82, 104–113. https://doi.org/10.1016/j.marpol.2017.05.014.

Tourrand, C., Naim, O., Bigot, L., Cadet, C., Cauvin, B., Semple, S., Montaggioni, L.F., Chabanet, P., Bruggemann, H., 2013. Fringing reefs of reunion island and eutrophication effects: PART 1: long-term monitoring of two shallow coral reef communities. Atoll Res. Bull. 596, 1–35. https://doi.org/10.5479/si.00775630.596.

Vanderstraete, T., Goossens, R., Ghabour, T.K., 2006. The use of multi-temporal Landsat images for the change detection of the coastal zone near, Hurghada, Egypt. In: International Journal of Remote Sensing. Taylor & Francis, pp. 3645–3655. https://doi.org/10.1080/01431160500500342.

Wilkinson, C., 2008. Status of coral reefs of the world: 2008. In: Global Coral Reef Monitoring Network and Reef and Rainforest Research Centre. Austral. Inst. Mar. Sci. (AIMS), Townsville, Australia, pp. 296.

Wilson, S.K., Graham, N.A.J., Polunin, N.V.C., 2007. Appraisal of visual assessments of habitat complexity and benthic composition on coral reefs. Mar. Biol. 151, 1069–1076. https://doi.org/10.1007/s00227-006-0538-3.

Windward Technologies, 1997. GRG2 Users's Guide.